Acta Geologica Polonica, Vol. 65 (2015), No. 2, pp. 181–203
DOI: 10.1515/agp-2015-0007

Epigenetic silicification of the Upper Oxfordian limestones in the Sokole Hills (Kraków-Częstochowa Upland): relationship to facies development and tectonics

JACEK MATYSZKIEWICZ[1], ALICJA KOCHMAN[*1], GRZEGORZ RZEPA[1], BOŻENA GOŁĘBIOWSKA[1], MARCIN KRAJEWSKI[1], KRZYSZTOF GAIDZIK[2, 3], JERZY ŻABA[2]

[1]*AGH University of Science and Technology; Faculty of Geology, Geophysics and Environment Protection, al. Mickiewicza 30; 30-059 Kraków, Poland. E-mail: jamat@geol.agh.edu.pl; *kochman@geol.agh.edu.pl; grzesio@geol.agh.edu.pl; goleb@uci.agh.edu.pl; kramar@geolog.geol.agh.edu.pl*
[2]*University of Silesia in Katowice, Faculty of Earth Sciences, ul. Będzińska 60; 41-200 Sosnowiec, Poland. E-mail: krzysztof.gaidzik@us.edu.pl; jerzy.zaba@gmail.com*
[3]*Departamento de Geografía Física, Instituto de Geografía, Universidad Nacional Autónoma de México, Ciudad Universitaria, Coyoacan, 04510 Mexico, DF, Mexico. E-mail: gaidzik@igg.unam.mx*

ABSTRACT:

Matyszkiewicz, J., Kochman, A., Rzepa, G., Gołębiowska, B., Krajewski, M., Gajdzik, K. and Żaba, J. 2015. Epigenetic silicification of the Upper Oxfordian limestones in the Sokole Hills (Kraków-Częstochowa Upland): relationship to facies development and tectonics. *Acta Geologica Polonica*, **65** (2), 181–203. Warszawa.

A spectacular epigenetic silicification was encountered in the Oxfordian bedded limestones exposed in the Sokole Hills situated in the Kraków-Częstochowa Upland. The main epigenetic mineral is microcrystalline quartz accompanied by minor goethite, hematite, barite, galena and sphalerite. Locally, the mineralized limestones reveal Pb and Cu contents exceeding over 150 times the background values of these metals in unmineralized limestones.

The epigenetic mineralization of the bedded limestones was probably a two-stage process. During the first, Early Cretaceous stage, silicified limestones formed at the erosional surface of a denuded carbonate complex. Such silicification greatly limited the progress of the first karstification phase of the Upper Jurassic carbonates initiated in the Hauterivian. The sources of silica accumulated in the limestones were descending solutions enriched in silica derived from the weathering zone. This silicification affected the topmost part of the Upper Jurassic massive limestones and the deeper portions of the bedded limestones along the fracture systems and stylolites.

Early Cretaceous tectonic activity generated new dislocations and re-opened the existing faults, which were subsequently filled with permeable Albian quartz sands. These openings became the migration pathways for ascending, warm, relict, sulphide-carrying hydrothermal solutions at the second formation stage of the epigenetic mineralization. The newly supplied silica from the Albian sands precipitated on the silicified limestones and, as concentric rims, on brecciated, early diagenetic cherts. The second-stage mineralization proceeded under phreatic conditions, presumably close to a fluctuating mixing zone of ascending, warm hydrothermal solutions and descending cold groundwaters. The brecciated cherts acting as silica crystallization nuclei indicate that the last mineralization stage probably followed the final phase of Cenozoic faulting.

Key words: Upper Jurassic limestones; Epigenetic silicification; Tectonic deformations; Kraków-Częstochowa Upland.

INTRODUCTION

The Kraków-Częstochowa Upland (KCU) belongs to the most spectacular areas in Europe where the Upper Jurassic (Oxfordian and Kimmeridgian) microbial-sponge and microbial carbonate facies (cf. Gwinner 1971) can be studied as the products of sedimentation along the vast, northern margin of the Tethys Ocean (Leinfelder 1993, 1996; Leinfelder *et al*. 1994). The KCU includes two geographical sub-units: the Kraków Upland and the Częstochowa Upland. Structurally, both units correspond to the area of the Silesian-Kraków Homocline built of Mesozoic formations (Żelaźniewicz *et al.* 2011; Text-fig. 1). The homocline rests upon

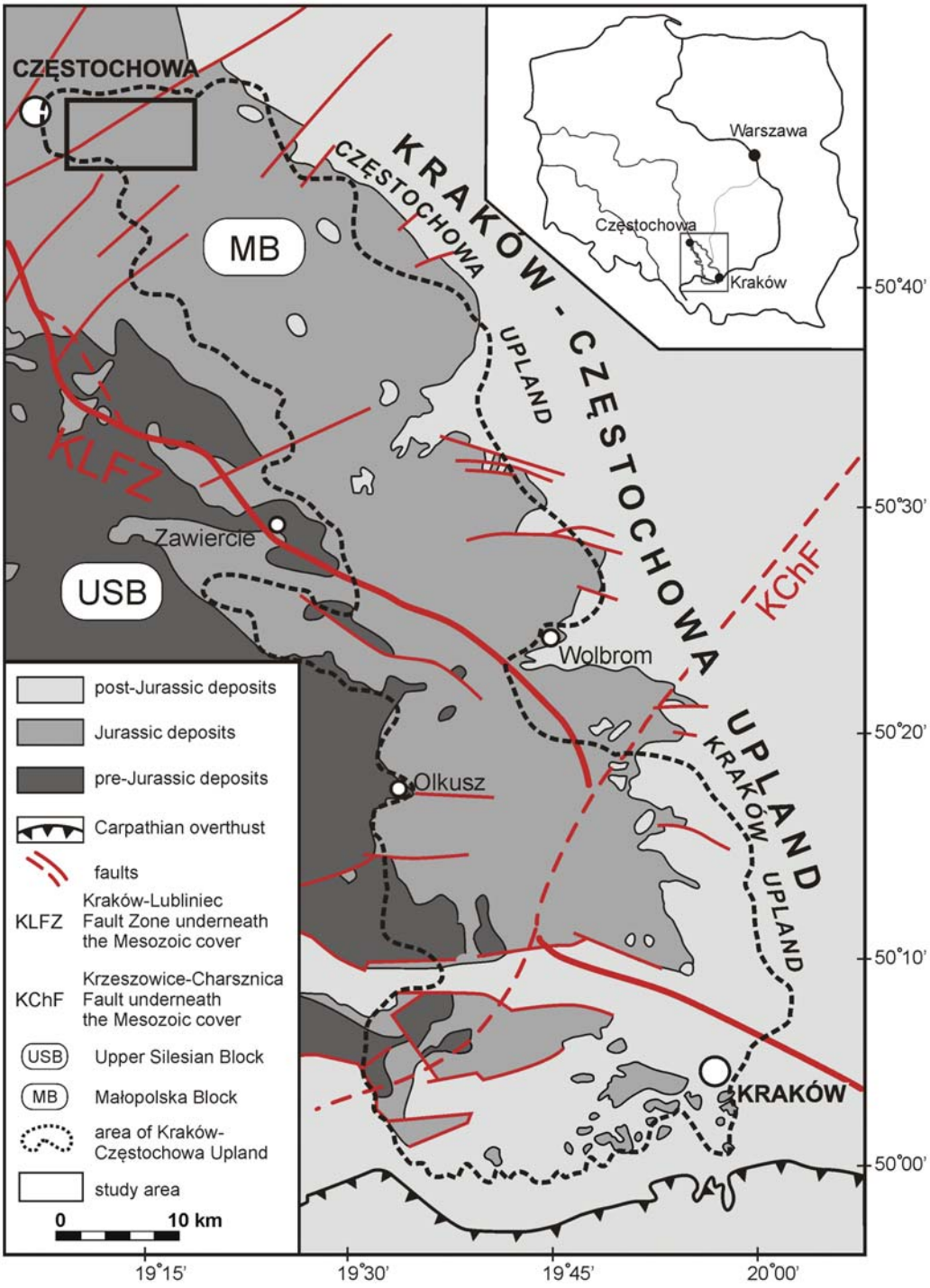

Text-fig. 1. Location map of the Sokole Hills against the geological setting of the Kraków-Częstochowa Upland (after Rühle *et al*. 1977; simplified)

folded Palaeozoic formations cut by the Kraków-Lubliniec Fault Zone (KLFZ), presumably a segment of the transcontinental Hamburg-Kraków Tectonic Line (Franke and Hoffman 1999) active since the Cambrian (Morawska 1997; Żaba 1999; Buła 2000, 2002).

Recently, the genetic links between the KLFZ and the significant facies diversity, as well as the epigenetic processes, in the overlying Upper Jurassic successions have been proposed. This was based especially on a vigorous growth of carbonate buildups in those parts of the Late Jurassic sedimentary basin that cover Permian magmatic intrusions localized in the basement along the KLFZ (Matyszkiewicz *et al*. 2006a), and on the influence of hydrothermal solutions on Upper Jurassic carbonates resting directly upon the KLFZ or in its vicinity (Pulina *et al*. 2005; Matyszkiewicz *et al*. 2006b; Kochman and Matyszkiewicz 2012). The action of warm, hydrothermal(?) solutions was also proposed to explain the origin of galena accumulations described from Upper Jurassic limestones located in the southern part of the Częstochowa Upland (Górecka and Zapaśnik 1981; Bednarek *et al*. 1985) and the formation of hypogenic karst caves discovered in some parts of the KCU (Żaba and Tyc 2007; Tyc 2009; Gradziński *et al*. 2009, 2011).

In the northern part of the KCU, there is a latitudinally extended chain of hills known as the Sokole (English: Falcon) Hills (Text-figs 1, 2). The hills are best known for the picturesque cliffs built of Upper Jurassic massive and bedded limestones with numerous karst features, including a number of hypogenic karst caves (Urban and Gradziński 2004; Gradziński *et al*. 2011). In the western part of the Sokole Hills, in the topmost portion of the Upper Jurassic succession, epigenetic mineralization was encountered as crusts composed of silicified and ferruginous limestones resting upon the Upper Jurassic bedded limestones and filling the joint systems, and faults cutting through the limestones. The present paper aims to explain the distribution pattern of the epigenetic mineralization and to prove its genetic link to tectonic deformations of the Sokole Hills related to the KLFZ.

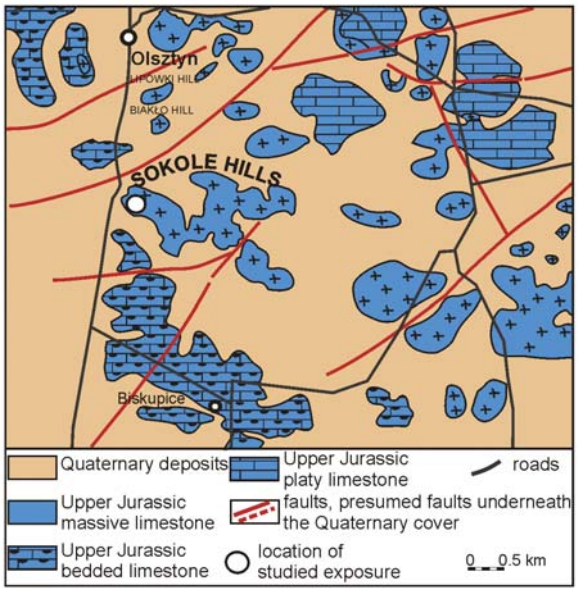

Text-fig. 2. Location of exposures of Oxfordian limestones in the vicinity of the Sokole Hills (after Heliasz *et al*. 1982; modified; cf. Text-fig. 1). The studied exposure is marked with an asterisk; the detailed distribution of limestone facies in its vicinity is shown in Text-fig. 4

GEOLOGICAL SETTING

The KCU is developed over the Silesian-Kraków Homocline, a regional tectonic unit built of Triassic, Jurassic and Cretaceous strata (Text-fig. 1). These rocks overlie unconformably folded Palaeozoic units of the West European Palaeozoic Platform. The Silesian-Kraków Homocline extends NNW–SSE, dipping at a low angle (several degrees) to the NE. Together with preserved fragments of Permian strata it constitutes the Permian-Mesozoic structural complex. The Silesian-Kraków Homocline started to form in the Early Cimmerian orogenic phase but its final structure was mostly the result of Cenozoic deformations.

The Palaeozoic formations underlying the homocline are cut by the KLFZ (Buła *et al*. 1997; Żaba 1999; Buła 2000, 2002). The KLFZ separates the Upper Silesian and the Małopolska tectonic blocks, two structural units located south-west of the East European Craton, within the Central European part of the West European Palaeozoic Platform (Dadlez *et al*. 1994). In the border zone between the Silesian and the Małopolska blocks, Lower Palaeozoic and older structural complexes are in direct contact. These units differ in lithology, age, character, intensity of deformation, and tectonic style (Żaba 1999; Buła 2002). The formation of uniform successions over both blocks started in the Early Devonian.

The activity of the KLFZ is closely connected with the Late Palaeozoic magmatism, particularly with granitoid plutons emplaced exclusively in the marginal part of the Małopolska Block. The course of the KLFZ shows numerous bends and arches, and its width usually does not exceed 500 m (Buła *et al*. 1997; Żaba 1999; Buła 2000, 2002). The zone has been active since the earliest Palaeozoic until Recent (Morawska 1997; Żaba 1999).

The Upper Jurassic formations of the Silesian-Kraków Homocline, which overlie the KLFZ or are located in its vicinity, host local accumulations of epige-

netic siliceous precipitates. Their distribution in the proximity of faults cutting through the Upper Jurassic limestones and/or on the locally preserved erosional surface capping the limestones has been known for a century (see Morozewicz 1909; Kuźniar and Żelechowski 1927; Różycki 1937; Dżułyński and Żabiński 1954; Alexandrowicz 1960; Bukowy 1960; Rajchel 1970; Łaptaś 1974; Heliasz 1980; Matyszkiewicz 1987). The origin of this mineralization is still controversial. The mineralization has been interpreted variously as: (i) the products of silica leaching from sandy sediments (so-called "moulding sands"; Gradziński 1977) and its subsequent migration (Różycki 1937; Bukowy 1960); (ii) Palaeogene weathering crusts covering the Jurassic carbonates (Alexandrowicz 1960; Rajchel 1970; Heliasz 1980); (iii) the products of Early Cretaceous weathering under subtropical conditions (Marcinowski 1970a, 1974; Głazek 1989; Głazek *et al*. 1992); and (iv) the precipitates of low-temperature hydrothermal solutions which migrated along the joint systems and faults generated during one of the tectonic episodes affecting the area (Morozewicz 1909; Kuźniar and Żelechowski 1927; Matyszkiewicz 1987).

The Sokole Hills are located in the northern part of the Częstochowa Upland, c. 10 km SE of Częstochowa (Text-figs 1, 2). This is a latitudinally extended chain of low hills, up to c. 400 m a.s.l., built of Upper Jurassic limestones that form characteristic tors, up to 20 m high. The hills are composed of massive limestone facies whereas the surrounding morphological depressions are incised in strongly fractured, bedded limestones with cherts. The massive limestones host numerous hypogenic karst caves formed in the Cenozoic by ascending, warm solutions (Gradziński *et al*. 2011). These solutions are also regarded as a source of numerous accumulations of coarse-crystalline calcite speleothems, which were occasionally mined in the past (Wójcik 2004; Gradziński *et al*. 2011).

The Upper Jurassic limestones exposed in the Sokole Hills are generally ascribed to the Oxfordian but their precise stratigraphic position is still unknown due to the lack of zonally significant ammonite faunas. Precise stratigraphic positioning in the Bifurcatus and Bimammatum zones has been made for limestones exposed in the vicinity of Olsztyn, c. 2 km north of the study area (Matyja and Wierzbowski 1992) and in the Biakło and Lipówki hills, c. 1 km north of the study area (Matyja and Wierzbowski 2006b; Text-fig. 2), but these sites are located behind the NE–SW-trending fault bordering the Sokole Hills to the north (Text-fig. 2). The Sokole Hills occupy the southern, downthrown block of the fault, with its vertical throw estimated between 40 and 160 m (Heliasz *et al.* 1987). Another fault of similar throw and W–E strike is known from the area immediately south of the Sokole Hills (Text-fig. 2; Heliasz *et al*. 1987).

Due to the lack of boreholes penetrating the Jurassic formation in the Sokole Hills, the thickness of the Upper Jurassic succession here could only be estimated as c. 150–200 m (after Heliasz *et. al*. 1982, 1987). Consequently, the Upper Jurassic stratigraphic column presented herein (Text-fig. 3) is rather hypothetical and is partly interpreted from data collected in the adjacent areas under two general assumptions: (i) high horizontal and vertical facies variability of the Oxfordian limestones; and (ii) a westward decrease in limestone thickness caused by erosional reduction of the homoclinally dipping Mesozoic formations. Facies variability of the Upper Jurassic limestones results from intensive growth of carbonate buildups controlled in the KCU area by local factors (Matyja and Wierzbowski 2006a; Matyszkiewicz *et al*. 2006a, 2012). In the Sokole Hills, the Upper Jurassic massive limestone facies forms the internal parts of the complex of microbial-sponge carbonate buildups whereas the bedded limestone facies with early diagenetic cherts occupy their slopes and local depressions. The central parts of vast depressions separating the buildups were presumably the sedimentary environment of platy limestones (Dżułyński 1952) but these rocks were already removed by erosion. The evolution of the carbonate buildups, from aggradational growth to lateral expansion, and their coalescence into large complexes were the factors controlling the formation of local sea-floor highs. From these highs, detrital material in the form of both episodic sliding of carbonate detritus and gravity flows was periodically transported downslope to deeper parts of the sedimentary basin. In the Oxfordian limestones exposed c. 5 km east of Częstochowa, Marcinowski (1970b) described calciturbidites that document the sea-floor relief at the end of the Oxfordian.

The Upper Jurassic succession of the Sokole Hills area (Text-fig. 3) begins with unexposed sponge limestones intercalated with marls, hosting abundant siliceous sponges, brachiopods, belemnites and ammonites. These strata, up to several metres thick, belong to the Cordatum Zone and are known as the Jasna Góra Beds (Trammer 1982). In the vicinity of Częstochowa, low-relief carbonate mud mounds, several metres high, are observed in these limestones (so-called "loose bioherms"; see Trammer 1982; Matyszkiewicz *et al*. 2012). Upsequence, pale coloured limestones appear, up to 70-80 m thick, locally named the Zawodzie Beds. In the lower part of the sequence, these limestones contain numerous tuberoids and cherts, either accumulated in horizons

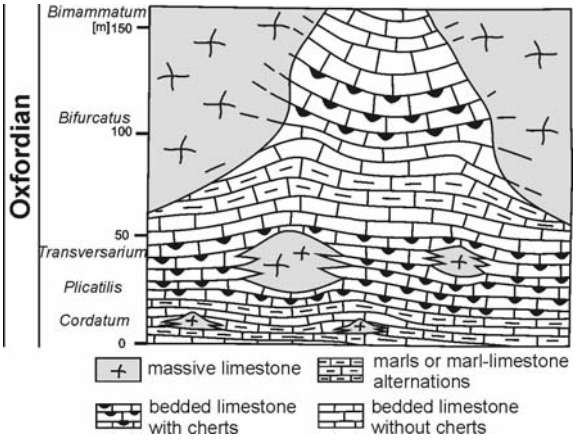

Text-fig. 3. Stratigraphic column of Oxfordian strata in the Sokole Hills (on the basis of Heliasz *et al*. 1982, 1987). Positions of ammonite zones are approximate

parallel to the bedding planes or randomly disseminated in the rock. Small initial carbonate buildups also appear locally (Heliasz *et al*. 1987). Towards the top of the sequence, the tuberoids disappear and thin (up to several centimetres thick) marly intercalations appear. These limestones span the Plicatilis through to the Bimammatum zones. The Zawodzie Beds are overlain by massive limestones, up to 20 m thick, locally intercalated with bedded detrital limestones with cherts of the Bimammatum Zone. They represent the microbial-sponge and microbial carbonate buildups regarded as agglutinated, microbial to open-space reefs (cf. Riding 2002; Matyszkiewicz *et al*. 2012).

In the exposures several km north-east of the study area, the succession is covered by Upper Oxfordian platy limestones, marls and chalky limestones, overlain by Kimmeridgian carbonates and by Albian (Cretaceous) quartz sandstones (Marcinowski 1970b, 1974). In the Sokole Hills, this cover was mostly removed by erosion and is only locally preserved at the erosional surface of the Oxfordian bedded and massive limestones.

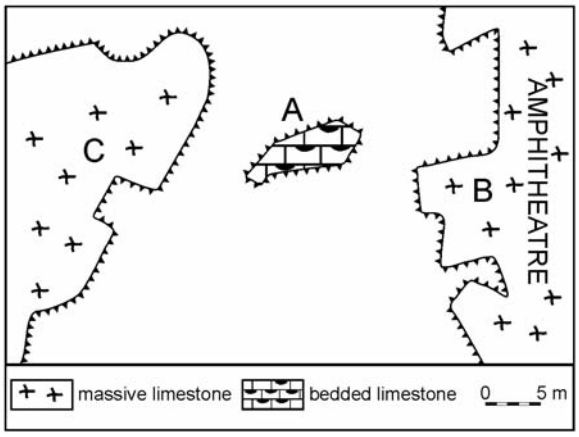

Text-fig. 4. Sketch map of the sites of epigenetic mineralization. A – tor built of bedded limestones with cherts and epigenetic mineralization. B – wall built of massive limestones with numerous karst caves ("The Amphitheatre"). C – outcrop of massive limestones

SECTION DESCRIPTION

The studied section with the epigenetic mineralization is located in a local morphological depression bordered to the east and west by towering high rocky walls (Text-fig. 4) with common karst caves (Text-fig. 5A). The formation of the caves took place during the Palaeogene or in the Miocene (Gradziński *et al*. 2011). The rocky walls are built mostly of massive, chert-free limestone. A 15-m-high eastern wall is called "The Amphitheatre". The western wall is c. 10 m high.

At the bottom of the Amphitheatre wall, karstified bedded limestones are visible, with bedding planes dipping to the west at 40°. To the east, they contact the massive limestones along a high-angle discontinuity surface which dips at 60° to the west. At the bottom of the massive limestones, bedded, chert-free limestone occurs locally. Its bedding planes dip at 20–30° to the ENE. The beds, up to 20 cm thick, are cut by dense kathetal fractures (Text-fig. 5B). In the bottom part of the massive limestones numerous calcified siliceous sponges are visible. Upsequence, the sponges are gradually replaced by microbialites.

At the edge of a tor located west of the described exposure, poorly bedded, chert-free limestones occur, with bedding planes dipping at about 20° to the WSW. Farther to the west, these limestones grade into massive limestones dominated in the bottom part by calcified siliceous sponges and in the top part by microbialites (similarly to the massive limestones from the Amphitheatre wall).

The exposure of epigenetic mineralization is located in the western part of a forested ridge of the Sokole Hills, c. 400 m of the local road from Biskupice to Olsztyn (Text-fig. 2). This is an isolated tor, c. 2.5 m high, and c. 5 m long in the N–S direction and c. 10 m in the W–E direction.

In the exposure, we observed a poorly bedded, fractured limestone with early diagenetic cherts distributed mainly close to the bedding planes (Text-fig. 6A). Limestone surfaces show numerous calcified siliceous sponges together with single brachiopods. Bedding planes dip at 10°–20° to the WNW or NW. The cherts are ellipsoidal concretions, up to 10 cm across and devoid of cracks, or elongated, horizontal bodies, up to 40 cm long and locally densely fractured.

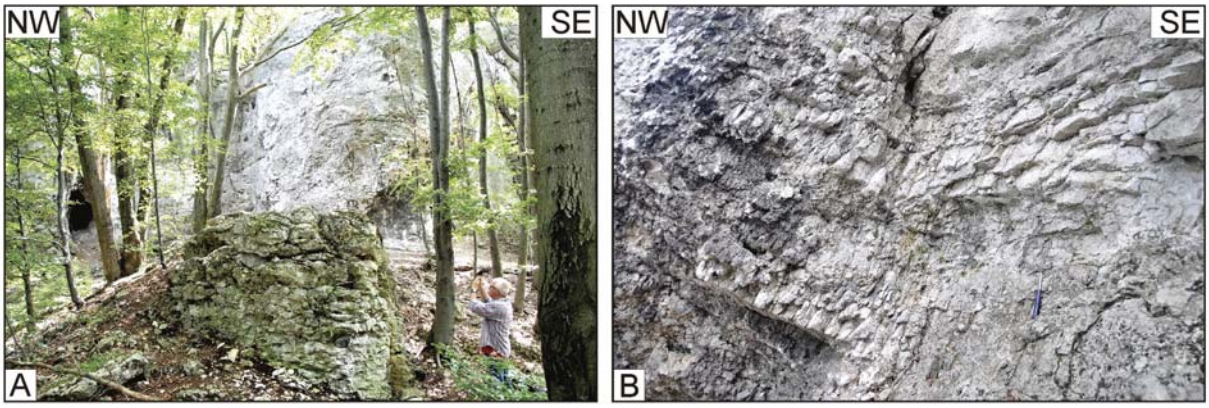

Text-fig. 5. Exposures of epigenetic mineralization in Upper Jurassic limestones. A – foreground: tor built of bedded limestone with epigenetic mineralization; background: rock wall built of massive limestone ("The Amphitheatre"; see Text-fig. 4); centre left: entrance to one of the numerous karst caves. B – lower part of the Amphitheatre built mostly of massive limestones; lower left: bedded limestone, free of cherts, with ENE-dipping bedding planes cut by numerous kathetal fractures. Inclination of bedding planes is of compactional character and resulted from the load that the already lithified carbonate buildup exerted on the unlithified bedrock

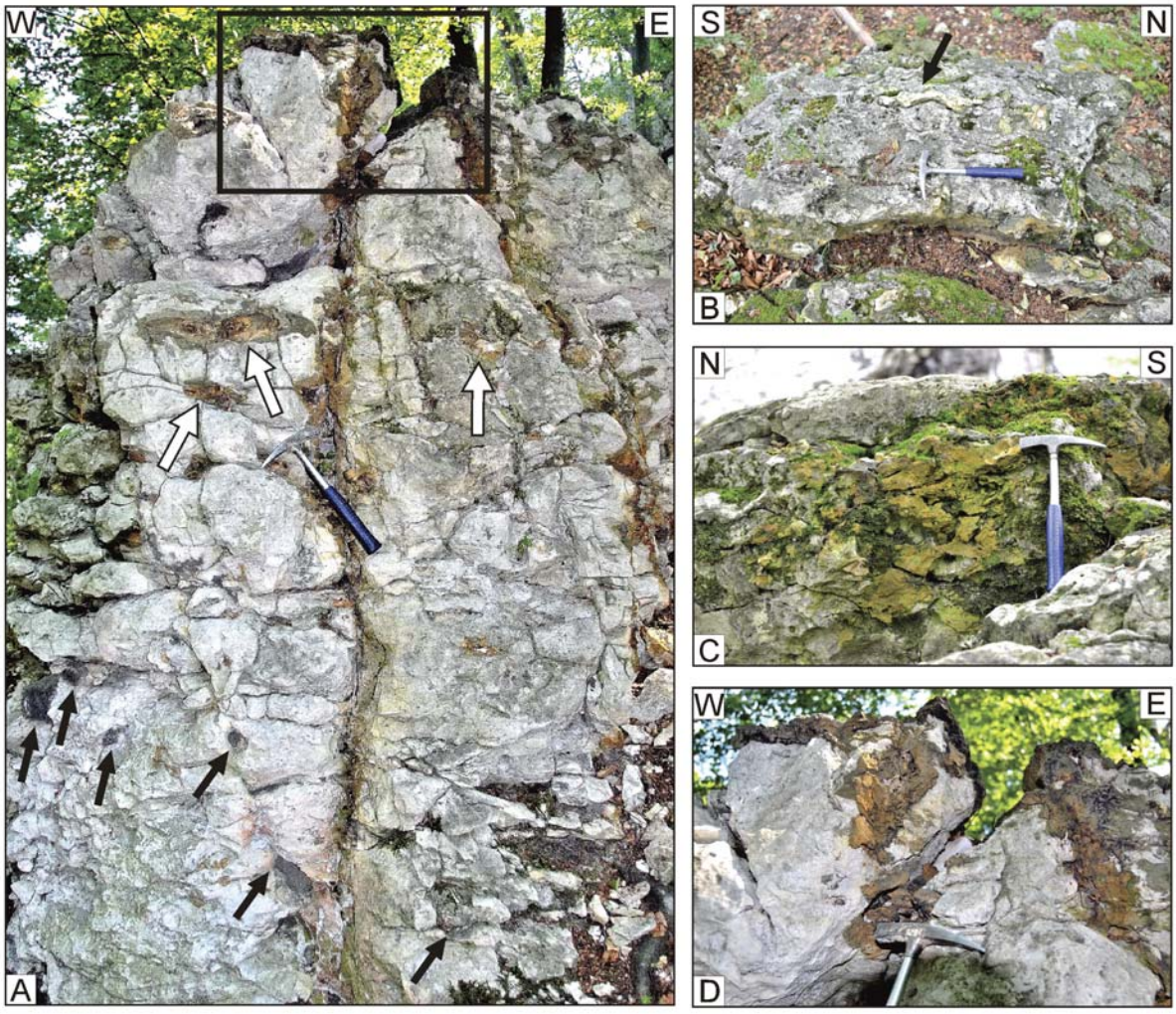

Text-fig. 6. Epigenetic mineralization in the tor built of bedded limestone with cherts (cf. Text-figs 4, 5A). A – bedded limestone with cherts (black arrows) and rims of silicified limestone enclosing the early diagenetic cherts (white arrows) cut by two high-angle fractures merging in the top of the tor. Fractures filled with epigenetic siliceous precipitates. Fragment in rectangle magnified in Text-fig. 6D. B – top surface of the tor. Open fissure seen in the lower part filled with epigenetic mineralization. Early diagenetic chert (arrow) elongated parallel to mineralized fissure. C – brownish, silicified limestone covering the surface of open fissure. D – crusts of epigenetic silica covering the top surface of the bedded limestone tor and the surfaces of the joint surfaces

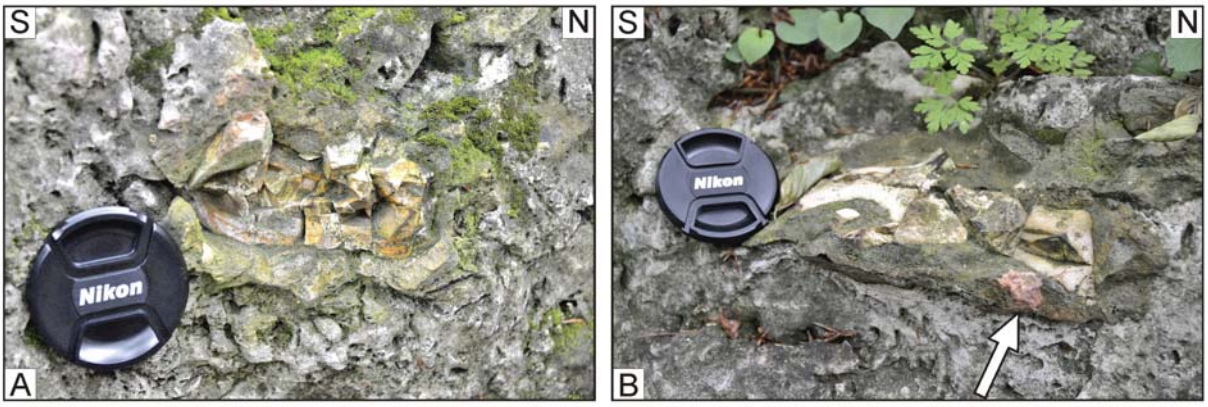

Text-fig. 7. Rims of silicified limestone enclosing the early diagenetic cherts, (probably the second stage of epigenetic silicification) in the rock wall bordering the exposure to the east (cf. Text-figs 4, 5A, 6). A – strongly fractured early diagenetic chert rimmed by unfractured, silicified limestone. B – brecciated early diagenetic chert with displaced fragments rimmed by grey, continuous zone of silicified limestone. In the bottom right fresh fracture of silicified rim about the reddish colour (arrow)

The early diagenetic cherts located close to the bedding planes sometimes show a NNE–SSW-trending elongation, parallel to the main joint systems observed in the limestones (Text-figs 6B, 7).

The bedded limestones host several fracture systems of various origins. Dominant are sub-vertical, NNE–SSW, NE–SW or, less commonly, NW–SE-striking fractures (Text-fig. 8). The first ones dip, most commonly, at a very high angle to the ESE or SE (Text-fig. 8B, max I: 124/85). This system controls the structural and morphological features of the limestones in the vicinity of the studied exposure. Moreover, a WNW–ESE system with several fracture sets was also identified (Text-fig. 8B). These are mostly vertical or very high-angle, NNE-inclined fractures, penetrating the whole area (Text-fig. 8B, max II: 210/85; Text-fig. 8C). Locally, we also found local sub-horizontal fractures dipping gently to the ESE or SE (Text-fig. 8B).

The southern side of the tor is cut by high-angle, upward-widening joints up to 20 cm wide in the top part (Text-fig. 6A–B). Along the joint walls several-cm-thick zones of epigenetic mineralization are developed as brown, yellow or reddish silicified limestones. The zones extend 2.5 m down the vertical, southern side (Text-fig. 6A) and can also be observed on the upper surface of the tor. A similar mineralized zone is visible locally on the western surface of the tor (Text-fig. 6C). The boundary between the silicified and unaltered parts of the limestones is sharp. Epigenetic silicification also occurs on the upper surface of the tor as a brown-reddish-yellow, porous crust, up to several cm thick (Text-fig. 6A, D). Finally, numerous fragments of silicified limestones are scattered in the weathering rubble, up to a dozen metres south of the tor.

Epigenetic silicification was also observed in the form of porous zones, up to 5 cm thick, rimming both the spheroidal and the flattened, early diagenetic cherts

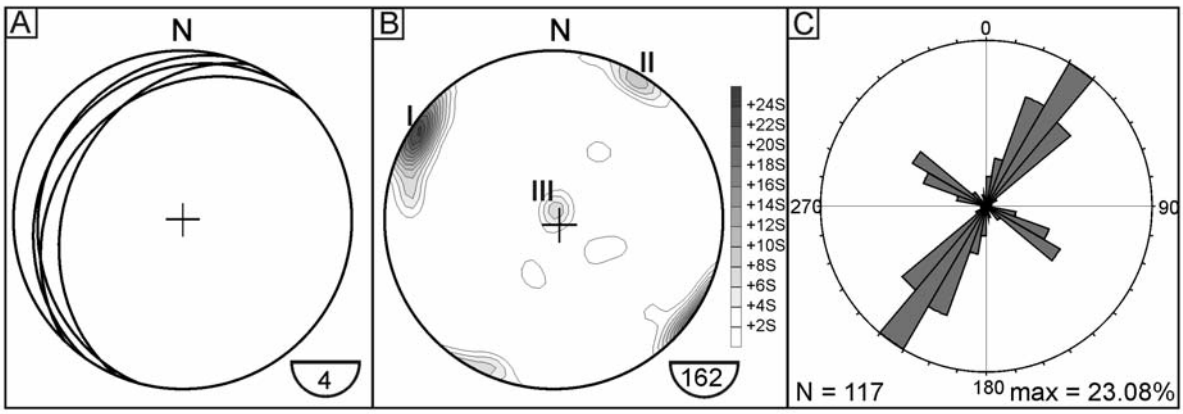

Text-fig. 8. Orientation diagrams of selected structures measured in exposed mineralized limestones of the central outcrop (outcrop A in Text-fig. 4). A – great circle arcs of bedding plane S_0. B – statistical contour diagram of poles to joints; main maxima: I – 124/85, II – 210/85, III – 162/5. C – rose diagram showing orientation variability of joints having dip angles over 50°

(Text-figs 6A, 7A, B) occurring close to the high-angle joints. Early-diagenetic, horizontally arranged cherts with silicified rims occur on the entire surface of the wall that cuts the exposure from the east and represents a high-angle joint (Text-fig. 7). The rims are continuous and massive whereas the enclosed cherts are strongly cracked.

Only on weathered surfaces do the silicified rims differ from both the silicified walls of joints and the silicified crusts covering the limestone beds in that they exhibit a grey colour, a regular, concentric shape and lower porosity (Text-fig. 7B). On the surfaces of fresh fractures, the silicified rims as well as other silicified limestones show the same yellow or reddish colour. The rims that developed around cherts located close to joints are wider than around those located in the bedded limestone where they disappear.

METHODOLOGY

In the studied exposure (Text-fig. 3), the main tectonic mesostructures were measured and sedimentary structures were documented, if visible, on the weathered limestone surface. From the silicified zones 30 samples were collected, mostly from the fillings of fractures located in the southern wall, from the crusts covering the top surface of the tor and rims developed on the cherts. Loose fragments of silicified limestones scattered in the rubble south of the tor were also taken. Five samples were collected from unaltered limestones encountered in the tor and in the western and eastern rock walls towering over the tor. From the collected samples polished and thin sections were prepared for microscopic examination and material was collected for chemical, Mössbauer, XRD, microprobe and isotope analyses, and for SEM studies. Samples were collected from hand specimens that differed macroscopically in colours and structural features. Chemical composition (main and trace elements) was analyzed at the Activation Laboratories in Ancaster (Canada) with the ICP-MS and ICP-EAS methods. Sample preparation included digestion of the material with a mixture of concentrated $HClO_4$, HNO_3, HCl and HF at 200°C to fuming and then dilution with *aqua regia*.

Phase composition was determined with X-ray diffractometry (XRD) in a Philips APD PW 3020 X'Pert instrument. Samples were ground in an agate mortar and analyzed under the following conditions: anode $Cu_{K\alpha}$, generator settings 35 kV and 30 mA, recording range 3–70°2Θ, step size 0.05°, counting time 1 second per step. The XRD patterns were interpreted with XRAYAN software using the diffraction patterns database of the International Centre for Diffraction Data.

The SEM–BSE observations and preliminary EDS analyses were carried out at the AGH University of Science and Technology, Kraków, using a FEI Quanta 200 FEG scanning electron microscope equipped with the EDS system. Sample selection was based upon observations under a binocular microscope. Natural, uncoated samples were studied under the low-vacuum mode (60 Pa pressure) whereas the polished sections were coated with graphite and observed under the high-vacuum mode.

The chemical composition of the silicified limestone was determined at the Inter-Institute Analytical Complex for Minerals and Synthetic Substances of the University of Warsaw with a Cameca SX 100 electron microprobe operating in wavelength-dispersive spectroscopic mode (WDS) under the following conditions: accelerating voltage 20 kV, beam current 15 nA, peak count-time 20 s, background time 10 s. The following set of standards, spectral lines and crystals was used: sphalerite: Zn (Kα, LIF), barite: Ba (Lα, PET), S (Kα, PET), chalcopyrite: Cu (Kα, LIF), Fe_2O_3: Fe (Kα, LIF), rhodonite: Mn (Kα, LIF), ZnSe: Se (Lα, TAP), galena: Pb (Mα, PET), CoO: Co (Kα, LIF), NiO (Kα, LIF), orthoclase: Al (Kα ,TAP), dioptase: Si (Kα, TAP), Ca_2SiO_4: Ca (Kα, PET), apatite: P (Kα, PET). Raw data were processes according to the "PAP" procedure (Pouchou and Pichoir 1985).

The Mössbauer spectroscopic analyses were completed using a Wissel 360 spectrometer and transmission method, at room temperature and at 77 K. The source was ^{57}Co placed in Rh matrix of 15 mCi activity.

Samples for Nd and Sm isotope analyses were taken from both the silicified and unaltered limestones, and analyzed at the Isotope Laboratory of the Adam Mickiewicz University in Poznań (Poland) with a Finnigan MAT 261 multi-collector thermal ionization mass spectrometer. Limestone samples were powdered and ~200 mg portions were weighed into 50 ml centrifuge tubes, treated with 5% ultra-pure acetic acid and mechanically shaken for 24 hours at room temperature (as recommended by Rongemaille *et al*. 2011). The solution obtained was then centrifuged in order to separate the acid-soluble fraction from the acid-insoluble residuum. In order to ensure the removal of all fine acid insoluble particles, the supernatant liquid was passed through a syringe filter with a 0.2 μm PTFE membrane. The filtered solution was equilibrated with a mixed ^{149}Sm-^{150}Nd tracer. The REE were stripped from the solution using the Fe hydroxide coprecipitation technique described by Fanton *et al*. (2002). The LREE were separated from matrix elements on 50 μl teflon columns filled with EICHROM TRU resin (see

Pin *et al*. 1994). Nd and Sm were then separated on 2 ml columns packed with Eichrom Ln resin. Nd and Sm (loaded as phosphate) were measured on Re in a double filament configuration. Isotopic ratios were collected in dynamic (Nd) and static (Sm) modes. During the analysis, the AMES standard yielded $^{143}Nd/^{144}Nd$ = 0.512129±7 (2σ mean of 19 analyses). The $^{143}Nd/^{144}Nd$ ratios were normalized to $^{146}Nd/^{144}Nd = 0.7219$, and the Sm isotopic ratios to $^{147}Sm/^{152}Sm = 0.56081$. Total procedure blanks were less than 35 pg for Nd and Sm. Nd isotope data were reported in the standard epsilon (ε) notation calculated using $^{143}Nd/^{144}Nd = 0.512638$ and $^{147}Sm/^{144}Nd = 0.1967$ for present-day CHUR (Jacobsen and Wasserburg 1980).

RESULTS

Microscopic studies

The Upper Oxfordian bedded limestones which host the epigenetic mineralization are wackestones-packstones with minor boundstones. In the wackestones-packstones, we observed tuberoids, fine intraclasts and abundant fragments of brachiopods, bivalves, bryozoans and benthic foraminifers. The main components of the boundstones are microbialites (stromatolites and thrombolites) with minor calcified spicules of siliceous sponges belonging to the Hexactinellidae. The calcified siliceous sponges together with epifauna attached to their bottom surfaces and microbialites overgrowing their upper surfaces form so-called "unitary sedimentary sequences" (cf. Gaillard 1983; Matyszkiewicz 1989). The space between the sponges is filled with fine-detrital wackestone-packstone. Stylolites are absent from the boundstones but occur in the wackestones-packstones, where they are usually filled with brownish Fe-oxides.

In the wackestones-packstones, the epigenetic mineralization occurs as impregnations of microcrystalline quartz. The silicification expands from the stylolites and fine joints into the rock mass (Text-fig. 9). Close to the stylolites and fine joints, alteration affects both the matrix and the embedded grains. Farther from the stylolites and joints, only the matrix is silicified whereas the larger grains remain unaltered. If silicification is complete the rock is porous. We found that pore walls of the silicified limestones can be: (i) stained with brownish Fe oxides (Text-fig. 9A); (ii) covered with a calcite film, up to 0.5 mm thick, (Text-fig. 9B); or (iii) covered with a thin (up to 0.1 mm) film of quartz microcrystals (Text-fig. 9C).

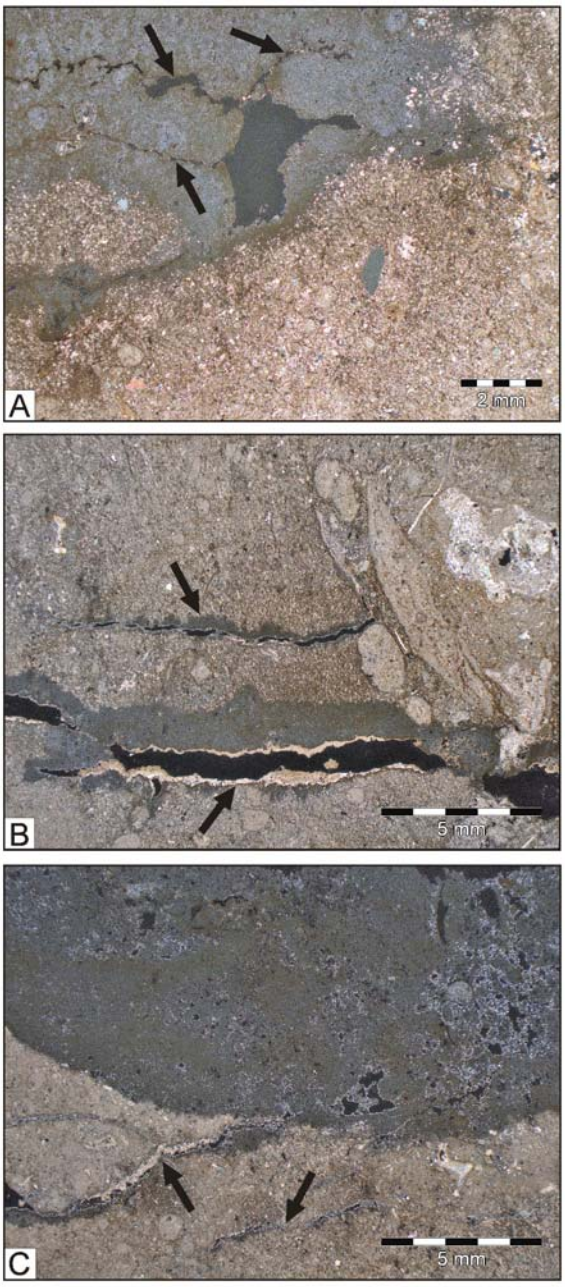

Text-fig. 9. Microfacies development of mineralized limestones. Optical microscope, polarized light, crossed nicols. A – upper part: entirely silicified, porous wackestone-packstone. Stylolites (arrows) extending from central cavity stained with brownish Fe oxides; lower part: packstone. Silicification altered only the matrix impregnated with Fe oxides. B – left and centre: packstone cut by solution-widened stylolites (arrows). Silicification proceeds from stylolites around which both the matrix and the larger grains are completely altered whereas deeper into the limestone only the matrix is silicified; bottom: stylolite stained with brownish Fe oxides and encrusted by young calcite crystals; right: boundstone free of stylolites and mineralized with impregnations of brownish Fe oxides at the edges of bioclasts and in surrounding, fine-detrital sediment. C – upper part: entirely silicified, porous packstone, walls of cavities encrusted with quartz crystals; lower part: selectively silicified packstone – only the matrix is replaced by epigenetic silica. Close to the stylolites (arrows) both the matrix and the larger grains are entirely silicified

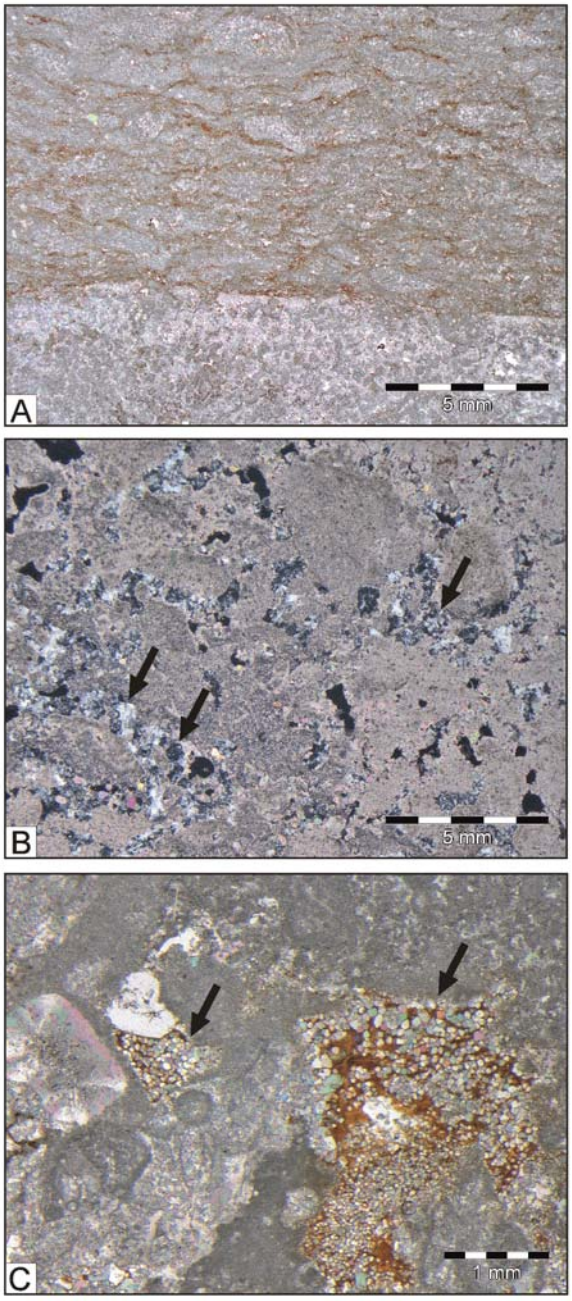

Text-fig. 10. Microfacies development of epigenetically mineralized massive limestones. Optical microscope, polarized light, crossed nicols. A – boundstone; upper part: microbialites growing on calcified siliceous sponge seen in the lower part of photograph. Outer laminae are covered with Fe oxides. B – boundstone; fragment of siliceous sponge. In some open spaces microflamboyant quartz is present (arrows), left after dissolution of primary, opaline skeletons of sponges. C – boundstone; small cavities (arrows) filled with aggregates of post-dolomite calcite crystals with Fe oxides

In the boundstones, the epigenetic mineralization in the unitary sedimentary sequences is poor and represented usually as brownish Fe oxides impregrations in outer films of layered thrombolites (Text-fig. 10A). Open spaces left after dissolution of opaline spicules of siliceous sponges are sometimes filled with megaquartz and microflamboyant quartz (Text-fig. 10B). In a single polished section, accumulations were observed in small cavities of fine (up to 0.1 mm across) post-dolomite calcite embedded within Fe oxides cement (Text-fig. 10C). In the wackestones-packstones that separate the unitary sedimentary sequences, silicification affects only the fine-crystalline matrix whereas the larger grains are unaltered.

SEM observations revealed the presence of euhedral quartz crystals in irregular cavities a few millimetres across scattered in the packstones in the silicified limestone (Text-fig. 11). Such quartz aggregates are commonly accompanied by accumulations of Fe oxide, up to 100 μm in size, in which we identified acicular iron oxide (probably goethite) crystals and Mn oxides together with rare, small, barite, galena and sphalerite crystals (Text-fig. 11) filling fine open spaces.

Mineralogical studies

The X-ray powder patterns support the microscope observations and indicate two main minerals in the analyzed samples: quartz and calcite (Text-fig. 12). Quartz was detected in all analyses but it tends to accumulate in the outer, more porous parts of the mineralized zones, where it is usually the only detectable mineral. In contrast, the calcite contents increase in the inner, more massive parts of the samples. The amounts of the Fe minerals goethite and hematite are low or even trace. Their spatial distribution is characteristic: goethite appears only in the yellow and brown zones (Text-fig. 12) whereas hematite occurs in reddish and cherry-red zones. Considering the variability of the colours of Fe minerals (Scheinost and Schwertmann 1999; Cornell and Schwertmann 2003), it is suggested that the yellowish zones consist of goethite and the reddish zones contain hematite.

Mössbauer analyses carried out for three zones of different colours in sample SG-12 (Text-fig. 12) from silicified limestone revealed the presence of only trivalent Fe, probably entirely bound in hydroxide minerals. In the red limestone hematite seems to be the only Fe mineral. The Mössbauer analyses indicated also the low level of magnetic ordering of the hematite, even at the temperature of liquid nitrogen (77 K), which demonstrates its low crystallinity (Cornell and Schwertmann 2003). In the yellow zones the main Fe carrier is goethite but an admixture of hematite is also possible.

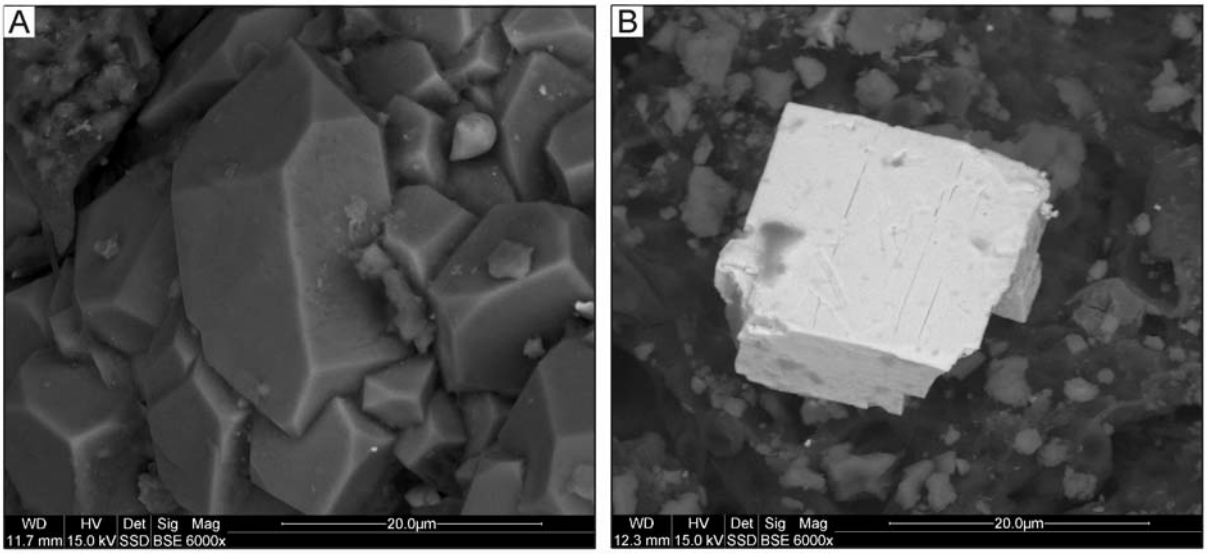

Text-fig. 11. SEM images of the products of epigenetic mineralization. A – euhedral quartz crystals; B – galena crystal

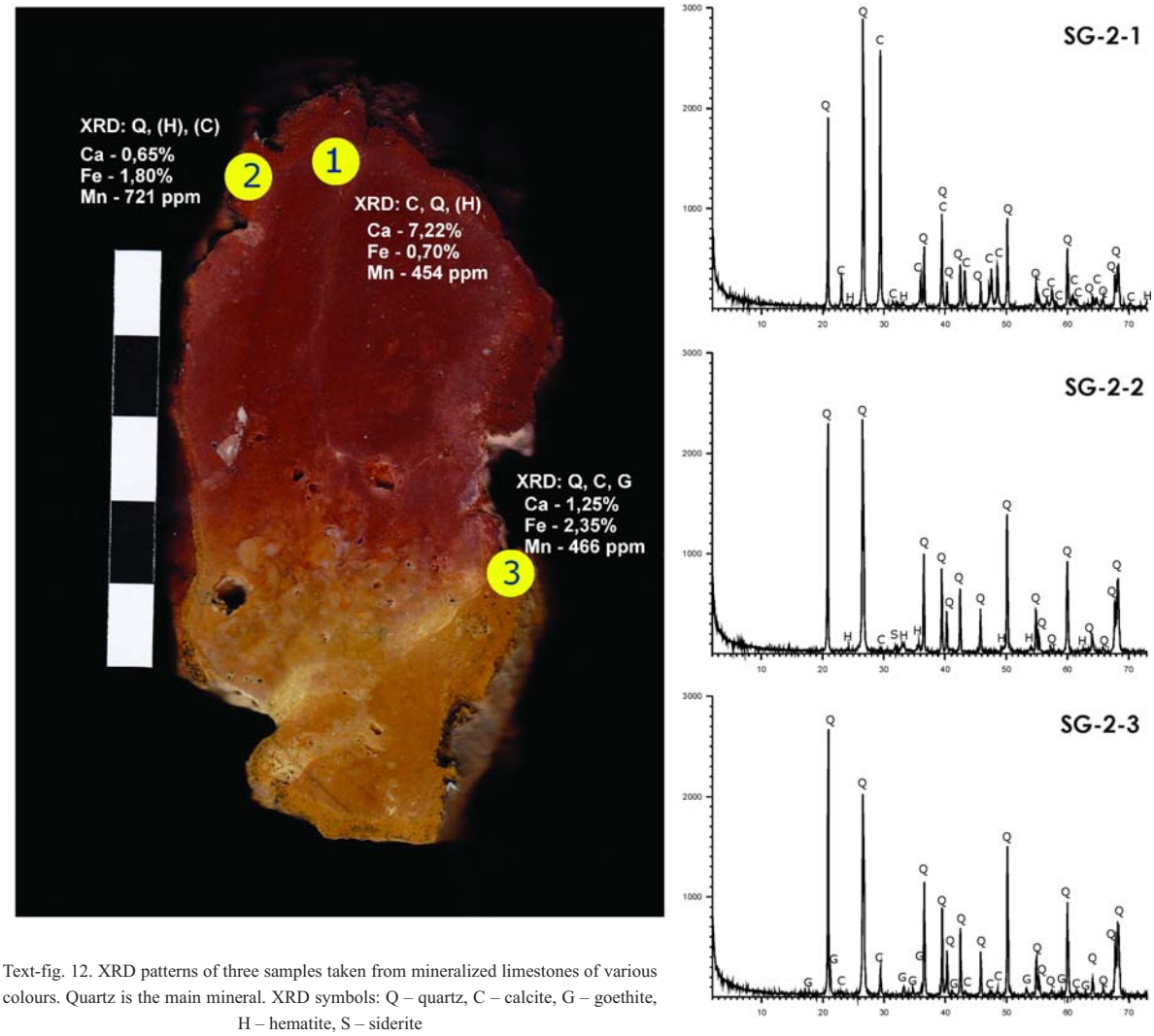

Text-fig. 12. XRD patterns of three samples taken from mineralized limestones of various colours. Quartz is the main mineral. XRD symbols: Q – quartz, C – calcite, G – goethite, H – hematite, S – siderite

Geochemical analyses

The contents of the main elements detected in the studied rocks are listed in Table 1. The CO_2 contents are extrapolated from the calcium values, assuming that all the Ca is bound in stoichiometric $CaCO_3$. These results are consistent with the X-ray powder patterns. The SiO_2 contents in the outer zones of epigenetic mineralization reach about 99 wt.% whereas the unaltered limestones contain only small amounts of SiO_2. The mineralized limestones also accumulate up to 6 wt.% of Fe_2O_3 (Table 1) while in the unaltered limestones the Fe_2O_3 contents are much lower. The contents of the remaining elements are below 1 wt.%. The contents of trace elements are variable (Table 2).

Microprobe analyses were made for interesting fragments of epigenetic mineralization hosted in the Oxfordian bedded limestones that differ in the BSE images. Point analyses show a few examples of increased contents of metals. The results of microprobe analyses indicated increased contents of Pb (up to 20 wt.%) in barite crystals. Sphalerite and galena grains (up to 20 μm across) (Text-fig. 8D) show traces of oxygen at the surface (up to 10 wt.%), which suggests weathering processes. The analyzed Fe oxides contain: Fe 48–61 wt.%, Si up to 8 wt.%, P about 2 wt.%, S 0.5 wt.%, Zn and Ca 1 wt.% , Ba and Al 0.5 wt.%. Some analyzed aggregates have also up to 7 wt.% Mn and traces of Ni, Co and Cu. Similarly to the Fe oxides, the Mn oxides fill minute cavities and cracks located in the silicified zone. Their composition includes: Mn 15–31 wt.%, Ca 10–28 wt.%, Fe and Al up to 4 wt.%, Ba up to 5 wt.%, Zn up to 1 wt.% and traces of Cu (up to 0.2 wt.%).

In most samples of the silicified limestones, increased contents of Ba, Cu, Pb, Sn, Zn, Ni, Co, Cr, V, As and Sb were detected. In some samples, Pb contents

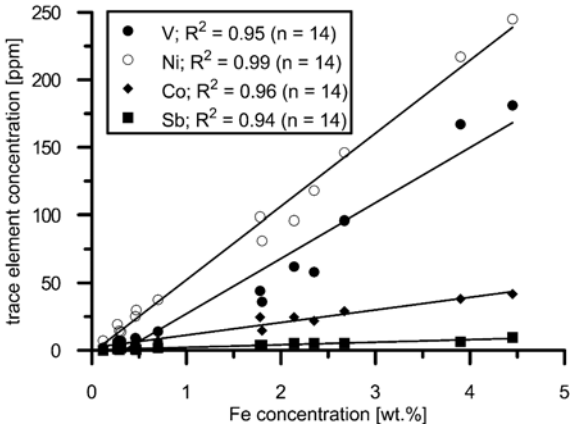

Text-fig. 13. Correlations between Fe and selected elements V, Ni, Co, and Sb in mineralized limestones; Fe versus V, Ni, Co, and Sb

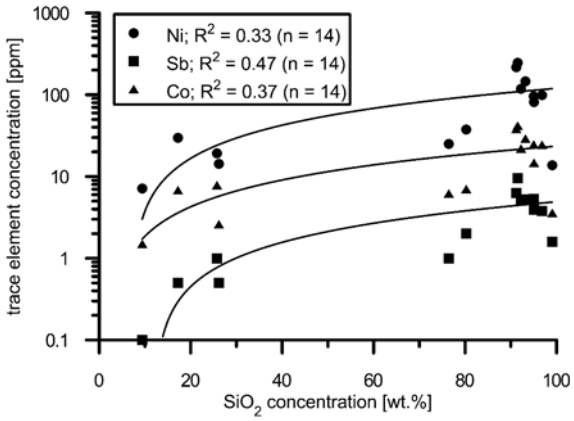

Text-fig. 14. Correlations between SiO_2 and selected elements in mineralized limestones; SiO_2 versus Ni, Sb and Co

are over 200 times higher (sample SG-D-1) and Cu ones are over 150 times higher (sample SG-12-3) than in the unaltered limestones. Samples rich in SiO_2 are evidently low in Sr (Table 2). The contents of Fe show strong correlation with the siderophile elements (Text-fig. 13), but only some elements show weak correlation with SiO_2 (Text-fig. 14). It is suggested that a direct genetic relationship occurs only between Fe and the siderophile elements, whereas a genetic link between Fe and SiO_2 is probably indirect.

Isotope analyses

The isotopic composition of Nd was analyzed in four samples of silicified limestone and in one unaltered limestone (Table 3). The result obtained for unaltered limestone ($\varepsilon_{Nd} = -6.6$) was calculated for the age of T=160 Ma (Oxfordian). For the silicified limestones, ε_{Nd} was additionally calculated for T=140 Ma (Berriasian/Valanginian), which is an assumed age of the beginning of epigenetic silicification, and for T=23 Ma (Oligocene/Miocene), which is an assumed age of the main faulting episode in the Kraków–Częstochowa Homocline.

DISCUSSION

The epigenetic mineralization hosted in the Oxfordian bedded limestones from the Sokole Hills formed at several stages determined by local and regional processes: (i) specific facies development of the limestones controlled by the depositional environment and compactional deformations affecting the limestones since their early diagenesis; and (ii) intensive weathering of the

Upper Jurassic complex in the Early Cretaceous under a subtropical climate and the subsequent ascent of warm solutions along the joint systems and faults.

(i) The bedded limestones that host the epigenetic mineralization were deposited in a local, narrow depression formed between microbial-sponge carbonate buildups which, over time, coalesced into a huge complex (Text-figs 4, 15A). It is possible that the thickness of this complex reached 500 m at the end of the Kimmeridgian, as shown by a borehole completed close to the Julianka Hill, about 15 km east of the Sokole Hills (Matyja and Wierzbowski 1996).

The main macroscopic differences between the massive and the bedded limestones are the presence of bedding planes and early diagenetic cherts in the bedded limestones. Moreover, the massive limestones contain more boundstones whereas the bedded limestones comprise more wackestones-packstones (cf. Matyszkiewicz 1989).

The differences in microfacies development of the massive and bedded limestones resulted in their differential diagenesis. In the early diagenesis, the main difference was silicification leading to the formation of early diagenetic cherts. The sources of silica were opaline spicules of sponges, which were particularly common in the bottom and middle parts of the buildups. After the death of organisms, the increasing pH controlled by decaying ectoderms facilitated the dissolution of metastable opaline spicules (cf. James *et al*. 2000). Initial dissolution of the sponge spicules took place in the topmost metres of the sediment and continued during shallow burial, probably to a depth of about 200–250 m (cf. Madsen *et al*. 2010). Remobilized silica migrated towards the local depression between the buildups (see e.g., Keupp *et al*. 1990; Lawrence 1994; Maldonado *et al*. 2005; Neuweiler *et al*. 2007). Silica then accumulated close to the initial stratification surfaces, forming plastic concretions that were fully lithified just when the first strike-slip deformations took place, perhaps with some contribution from meteoric waters (cf. Knauth and Epstein 1976; Knauth 1979; Kolodny *et al*. 1980; Bustillo *et al*. 1998) or even under hydrothermal influence (cf. Jones and Jenkyns 2001; Migaszewski *et al*. 2006; Coimbra *et al*. 2014). The quartz crystallinity index (CI; Murata and Norman, 1976) of the Oxfordian early diagenetic cherts from the southern part of the KCU is lower than 1.0, which indicates that their origin differs from that of the epigenetic siliceous deposits, for which the CI values vary from 9.2 to 9.9 (Matyszkiewicz 1987).

The ε_{Nd}=−6.6 value obtained for the unaltered limestones seems to preclude the action of solutions originating from sea-floor hydrothermal activity linked to extensional tectonics. According to Stille *et al*. (1996), the Tethys ocean between 170 and 150 Ma ago had Nd isotopic signatures ε_{Nd}=−6, but with the subsequent plate movement continental runoff became more important and led to a decrease in Nd isotopic values. The ε_{Nd}=−6.6 value for the unaltered Oxfordian limestones probably resulted only from the erosion of continental crust and the climatic conditions.

Both limestone facies from the Sokole Hills revealed different rates of lithification. The boundstones

	SG-W	SG-2-1	SG-2-2	SG-2-3	SG-C-1	SG-C-2	SG-C-3	SG-D-1	SG-12-1	SG-12-2	SG-12-3	SG-12-4	SG-12-5	SG-12-6
SiO_2	9.40	80.28	95.07	92.24	99.04	96.83	76.45	95.03	26.18	17.20	25.73	91.19	93.20	91.52
TiO_2	0.00	0.01	0.01	0.02	0.01	0.02	0.00	0.07	0.01	0.00	0.01	0.01	0.01	0.01
Al_2O_3	0.08	0.15	0.23	0.43	0.13	0.15	0.08	0.70	0.11	0.06	0.08	0.30	0.15	0.26
Fe_2O_3	0.17	1.00	2.57	3.36	0.44	2.55	0.66	3.06	0.41	0.67	0.39	5.58	3.82	6.36
MnO_2	0.02	0.07	0.11	0.07	0.01	0.01	0.01	0.01	0.03	0.03	0.03	0.04	0.02	0.03
CaO	50.12	10.11	0.91	1.75	0.14	0.13	12.57	0.36	40.60	45.50	40.88	1.43	1.46	0.84
MgO	0.25	0.05	0.02	0.03	< 0.01	< 0.01	0.08	0.05	0.17	0.22	0.22	0.03	0.02	< 0.01
Na_2O	< 0.01	< 0.01	< 0.01	< 0.01	< 0.01	0.01	< 0.01	0.03	0.01	< 0.01	< 0.01	0.01	< 0.01	< 0.01
K_2O	0.01	0.02	0.04	0.06	0.04	0.04	0.02	0.10	0.02	< 0.01	0.01	0.06	0.02	0.04
SO_3	0.55	0.15	0.03	0.05	0.05	0.10	0.18	0.13	0.48	0.53	0.50	0.05	0.03	0.03
P_2O_5	0.02	0.21	0.30	0.60	0.02	0.07	0.06	0.18	0.08	0.03	0.05	0.17	0.14	0.25
CO_2	39.38	7.94	0.72	1.38	0.11	0.10	9.88	0.29	31.90	35.75	32.12	1.12	1.14	0.66

Table 1. Contents of main elements in mineralized Oxfordian limestones from the Sokole Hills (in wt.%). Sample W is an unaltered limestone

	SG-W	SG-2-1	SG-2-2	SG-2-3	SG-C-1	SG-C-2	SG-C-3	SG-D-1	SG-12-1	SG-12-2	SG-12-3	SG-12-4	SG-12-5	SG-12-6
Ag	0.17	< 0.05	< 0.05	< 0.05	< 0.05	< 0.05	< 0.05	0.33	0.09	0.08	0.21	0.16	0.11	0.07
As	3.3	4.0	7.9	10.7	6.2	17.8	5.5	34.2	1.3	2.2	1.2	20.4	16.4	21.0
Ba	4	46	89	68	75	54	6	173	13	4	77	21	21	18
Be	< 0.01	0.2	0.3	0.4	0.2	0.3	0.2	0.5	0.1	0.1	< 0.1	0.6	0.5	0.7
Bi	0.12	0.06	0.09	0.09	0.22	0.23	0.02	1.16	0.04	< 0.02	0.09	0.11	0.10	0.18
Cd	0.4	1.0	1.4	2.3	0.1	0.2	0.6	1.1	0.8	0.5	0.7	0.7	0.5	1.1
Ce	1.8	1.9	1.9	2.7	0.7	0.9	1.3	3.8	2.2	2	2.6	1.7	0.9	1.4
Co	1.5	7	14.7	21.9	3.6	24.5	6.2	24.6	2.6	6.8	7.8	38.1	29	41.8
Cr	2.8	6.9	17.1	11.6	11.2	31.8	10.7	21.0	2.1	4.1	5.2	82.7	51.7	40.9
Cs	0.17	0.25	0.47	1.2	0.3	0.22	0.1	1.04	0.22	0.09	0.17	0.51	0.19	0.31
Cu	6.5	16.8	18.2	43.8	6.5	34.1	11.3	85.1	5.0	5.9	993.0	73.5	43.9	80.2
Dy	0.5	0.5	0.3	0.4	< 0.1	< 0.1	0.3	0.4	0.7	0.8	1.1	0.3	0.2	0.4
Er	0.4	0.2	0.2	0.3	< 0.1	< 0.1	0.2	0.2	0.4	0.6	0.7	0.2	0.1	0.3
Eu	0.08	0.1	0.08	0.09	< 0.05	< 0.05	0.06	0.08	0.17	0.17	0.19	0.07	< 0.05	0.08
Ga	0.1	0.6	0.7	1.1	0.7	1.3	0.5	3.5	0.2	0.1	0.2	2.1	1.3	2.3
Gd	0.5	0.6	0.4	0.5	< 0.1	< 0.1	0.3	0.4	0.9	0.9	1.2	0.3	0.2	0.4
Ho	0.1	< 0.1	< 0.1	< 0.1	< 0.1	< 0.1	< 0.1	< 0.1	0.1	0.2	0.2	< 0.1	< 0.1	< 0.1
La	4.1	3.2	2.6	3.1	0.5	0.7	2.2	2.4	5.9	6.1	7.2	1.9	1.2	1.9
Li	0.9	4.9	5.0	6.3	5.0	5.9	3.7	6.9	2.8	0.7	2.9	6.8	4.8	8.4
Mn	132	454	721	466	33	48	85	91	164	212	168	223	142	164
Mo	0.2	0.3	0.6	0.6	1.3	0.8	0.5	1.1	< 0.1	0.3	< 0.1	1.2	1.1	1.2
Nb	0.1	0.2	0.3	0.4	0.2	0.2	< 0.1	0.9	0.1	< 0.1	0.1	0.4	0.2	0.4
Nd	2.0	2.4	1.8	2.2	0.4	0.5	1.4	2.0	3.7	3.6	4.3	1.3	0.9	1.5
Ni	7.1	37.5	81	118	13.7	98.7	25.1	96	14.3	29.8	19.2	217	146	245
Pb	1.4	7.1	13.1	14.5	60.2	66.3	2.8	340	3.4	1.3	32	12.6	12.3	16.5
Pr	0.5	0.6	0.5	0.5	0.1	0.1	0.3	0.5	0.8	0.9	1.0	0.3	0.2	0.3
Rb	1.0	2.4	4.9	10.6	2.4	2.5	1.3	7.5	1.6	0.5	1.3	4.5	2.7	3.3
Re	0.001	0.002	< 0.001	0.002	0.001	0.002	0.004	0.002	0.001	0.003	0.003	< 0.001	0.001	0.002
Sb	0.1	2.0	3.9	5.2	1.6	3.8	1.0	5.3	0.5	0.5	1.0	6.3	5.2	9.5
Se	0.6	0.7	0.6	< 0.1	0.8	0.1	0.1	0.2	0.5	< 0.1	0.2	1.0	0.4	0.5
Sm	0.3	0.5	0.3	0.4	< 0.1	< 0.1	0.3	0.4	0.7	0.7	0.8	0.3	0.2	0.3
Sn	0.5	2	< 1	3	2	1	< 1	6	< 1	< 1	11	< 1	1	< 1
Sr	109	15.4	5	7.5	2.7	2.7	29.3	12.1	60.7	111	91	4.2	5.9	3.6
Tb	< 0.1	< 0.1	< 0.1	< 0.1	< 0.1	< 0.1	< 0.1	< 0.1	0.1	0.1	0.2	< 0.1	< 0.1	< 0.1
Te	< 0.1	0.2	< 0.1	0.3	0.1	0.5	0.2	0.3	0.2	0.1	< 0.1	0.5	0.2	0.4
Th	0.1	0.2	0.3	0.4	0.1	0.2	0.1	1	0.2	< 0.1	0.1	0.4	0.2	0.3
Tl	< 0.05	0.06	0.12	0.2	0.21	0.12	0.06	0.39	< 0.05	< 0.05	< 0.05	0.09	0.05	0.07
U	0.2	< 0.1	< 0.1	0.1	< 0.1	< 0.1	< 0.1	0.4	0.2	0.2	0.3	0.1	< 0.1	0.1
V	2	14	36	58	7	44	9	62	5	8	6	167	96	181
W	< 0.1	0.1	0.2	0.4	0.3	0.4	0.1	1.1	0.1	< 0.1	7.9	1	0.7	1.2
Y	7.6	4.3	3.5	3.7	0.5	0.7	2.9	2.4	7.2	8.4	12.8	3.0	2.2	3.9
Yb	0.3	0.2	0.2	0.2	< 0.1	< 0.1	0.2	0.2	0.3	0.4	0.5	0.2	0.1	0.2
Zn	25.7	114	236	392	50.5	221	89.8	308	49.5	54.1	566	398	286	463
Zr	< 1	2	2	3	2	3	2	5	1	2	2	5	3	5

sample	weight [mg]	$^{143}Nd/^{144}Nd$ (T=0)	ε_{Nd} (T=0)	$^{143}Nd/^{144}Nd$			ε_{Nd}			$^{147}Sm/^{144}Nd$	Nd [ppm]	Sm [ppm]	Sm/Nd	T_{2DM} [Ga]
				T=155 Ma	T=145 Ma	T=23 Ma	T=155 Ma	T=145 Ma	T=23 Ma					
SG-12	146.52	0.512207	-8.4	0.512098	0.512105	0.512191	-6.7	-6.8	-8.1	0.1084	2.71	0.49	0.18	1.49
SG-B	96.56	0.512198	-8.6	0.512087	0.512094	0.512182	-6.9	-7.0	-8.3	0.1101	2.34	0.43	0.18	1.50
SG-D	167.85	0.512223	-8.1	0.512114	0.512121	0.512207	-6.3	-6.4	-7.8	0.1077	2.08	0.37	0.18	1.49
SG-E	179.49	0.512226	-8.0	0.512119	0.512126	0.512226	-6.2	-6.4	-7.8	0.1060	1.67	0.29	0.18	1.46
SG-W	187.27	0.512208	-8.4	0.512099			-6.6			0.1076	1.71	0.31	0.18	1.45

Table 3. Results of Nd isotopic analysis of Oxfordian limestones. T values assumed for ε_{Nd} calculations: T=160 Ma for unaltered Oxfordian limestone, T=140 Ma (Berriasian/Valanginian boundary) and T=23 Ma (Oligocene/Miocene boundary) for mineralized limestones respectively. Sample W is an unaltered limestone

of the massive facies were subjected to intensive, synsedimentary cementation (cf. Riding 2002; Matyszkiewicz *et al*. 2012), whereas lithification lasted much longer in the fine-grained, porous wackestones-packstones that prevailed in the bedded limestones.

Important differences appeared also during burial diagenesis. Intensive growth of the carbonate buildups resulted in their increasing thickness. Hence, at the end of the Kimmeridgian, the lower portions of the Sokole Hills buildups were buried under at least 250–300-m-thick overburden (Text-fig. 15A), and the pressure from such a load became sufficient to initiate chemical compaction (Schlanger and Douglas 1974; Garrison 1981; Czerniakowski *et al*. 1984). Early diagenetic cementation of the boundstones significantly reduced the stylolitization of the massive limestones, while the pressure-solution processes initiated in the bedded limestones led to the formation of lithostatic stylolites and to some reduction in the thickness of the sediment (cf. Matyszkiewicz 1999; Kochman and Matyszkiewicz 2013). However, the intensity of pressure solution in the bedded limestones was insufficient to produce the so-called "pseudonodular limestones" (cf. Matyszkiewicz 1994).

The initial surfaces of primary stratification, which then evolved into the bedding planes, probably appeared at a synsedimentary stage. During burial diagenesis in the Late Jurassic, after the main phase of mechanical compaction (cf. Kochman and Matyszkiewicz 2013) but prior to full lithification of the carbonate sediments, cherts formed concordantly to these surfaces. The increasing load from the growing carbonate buildups resulted in compactional bending of the limestone beds underlying the buildups (Text-fig. 5B).

The above-discussed differences in the presence of bedding planes, microfacies and intensity of stylolitization of both limestone facies caused the bedded limestones to be more susceptible to epigenetic silicification. During this alteration, the fine-grained carbonate matrix in the wackestones-packstones was replaced by microcrystalline, granular quartz (Text-fig. 9) precipitated from solutions migrating along the erosional surface and/or along the joints systems, faults and stylolites.

(ii) Between the Tithonian and the Valanginian, the Upper Jurassic complex was subjected to intensive weathering and denudation under a subtropical, savannah-like climate and low relief landscape stability conditions (Marcinowski 1970a, 1974; Głazek 1989). Weathering and denudation of the Upper Jurassic sediments reduced their thickness in the Sokole Hills area by at least 250–300 m (Text-fig. 15B). It is probable that an extensive duricrust (?pedogenic silcretes) de-

Table 2. Contents of trace elements in mineralized Oxfordian limestones (in ppm). Sample W is an unaltered limestone

veloped in the top part of the Upper Jurassic limestones (Marcinowski 1970a, 1974; Głazek 1989; Głazek *et al*. 1992) during this time, for which the silica was supplied from the weathering crusts (cf. Milnes and Thiry 1992; Nash *et al*. 1998; Ullyott and Nash 2006). The silicification proceeded in a vadose zone unfavourable for deep groundwater circulation (Głazek 1989; Głazek *et al*. 1992; cf. Thiry and Milnes 1991; Dixon and McLaren 2009; Bustillo *et al*. 2013) as an effect of descending solutions enriched in dissolved silica. This silica presumably originated from long-lasting (Thiry 1999) leaching of opal (cf. Mišik 1996). Silicification of the bedded limestones progressed not only from the top surface of the carbonate succession but also from the joint systems and stylolites (Text-fig. 9A–C), which became conduits for the transfer of mineralizing solutions (cf. Braithwaite 1989; Matyszkiewicz 1994).

The hard, silicified limestones covered vast areas occupied by weathered Upper Jurassic limestones and reduced their karstification – a process initiated in the Hauterivian (Głazek *et al*. 1992). The different lithologies of the limestone facies and the resulting differential susceptibility to tectonic deformation are probably reflected by the different thicknesses of the silicified crusts generated over the massive and the bedded limestones respectively. The topmost part of the massive limestones was silicified to only shallow depths, and most of these silcretes might have been eroded during the Cenozoic karstification followed by the Quaternary weathering. In the case of the bedded limestones, on the other hand, penetration of the mineralizing solutions was much deeper because alteration proceeded from the upper surfaces of the limestone beds, from stylolites (Text-fig. 9) and from joints (Text-figs 6, 7). Hence, much thicker crusts were generated and the chances of their preservation became much higher. That is why the epigenetic siliceous precipitates preserved in the KCU occur almost entirely in the topmost parts of the faulted bedded limestones (cf. Matyszkiewicz 1987).

The development of the epigenetic siliceous rocks from the Sokole Hills resembles that of the geologically similar, Lower Cretaceous silcretes-ferricretes described by Azmon and Kedar (1985) from the Maktesh Gadol area in Israel. The bulk of the rock may appear to be ferruginized even to ore grade but, in fact, it is only a silicified limestone with the ferruginization limited mostly to a brown-reddish-yellow colour. Moreover, both the composition and geochemistry of the siliceous precipitates from the Sokole Hills (Table 1) are incompatible with typical pedogenic silcretes, which show a high TiO_2 content (cf. Milnes and Thiry 1992; Thiry and Simon-Coinçon 1996; Nash *et al*. 1998; Ullyot and Nash 2006; Tofalo and Pazos 2010; Bustillo *et al*. 2013).

It seem improbable that descending silicification of the limestones might have produced detectable enrichments of rocks in Ba, Cu, Pb, Sn, Zn, Ni, Co, Cr, V, As and Sb (Table 2) although weathering processes might have slightly increased the contents of Cr, Zn, Cd and Pb (Ni *et al*. 2009). The correlations of Fe contents with V, Ni, Co and Sb (Text-fig. 13) as well as those of SiO_2 with Ni, Co, Sb, Cr, V and As (Text-fig. 14) suggest the supply of trace elements from ascending solutions. The highly increased amounts of Pb and Cu detected in some samples might have resulted from the local action of relict hydrothermal fluids, probably related to one of the deformation stages (cf. Bruhn *et al*. 1994; Sibson 1987; Aranburu *et al*. 2002). Similarly, the presence of Zn and Pb sulphides, and the admixtures of both elements in Fe and Mn oxides together with the observed Pb-barite and euhedral quartz crystals (Text-fig. 11) allow us to conclude that the epigenetic mineralization could not have been emplaced exclusively during pedogenesis under a subtropical climate, and that penetration of the top surface of the bedded limestones by descending, silica-rich solutions but it must have been supplemented by ascending, warm, hydrothermal fluids. Weak correlation between Fe and SiO_2 suggests that crystallization of Fe dioxides and sulphides probably preceded the next stage of epigenetic silicification.

The results of Nd isotope analyses of the epigenetically silicified limestones from the Sokole Hills (Table 3), recalculated to a depositional age of T=140 Ma (Berriasian/Valanginian), range between –7.0 and –6.4, which roughly correspond to the formation time of the silcretes and precludes the contribution of hydrothermal solutions derived from deep mantle sources (cf. Stille and Fischer 1990; Stille *et al*. 1989, 1996; Pucéat *et al*. 2005). At this time, the Tethys seawater almost reached its continental crust-like, lowest Nd isotopic composition values. The ε_{Nd} values obtained for the silicified limestones probably result only from mechanical erosion of continental crust (cf. Stille *et al*. 1996). We believe that, after the formation of the incipient silcretes, the second, phreatic stage of epigenetic alteration commenced. It was related to the action of ascending, warm solutions, which migrated along numerous joints and faults filled with permeable Albian quartz sands (Text-fig 15C). This second stage was similar to the origin of the so-called "groundwater silcretes" or "drainage-line silcretes" (cf. Milnes and Thiry 1992; Nash *et al*. 1998), which are characterized by a limited range and a high precipitation rate (Thiry 1988). The ascending, warm solutions probably mixed with cold groundwaters saturating the quartz

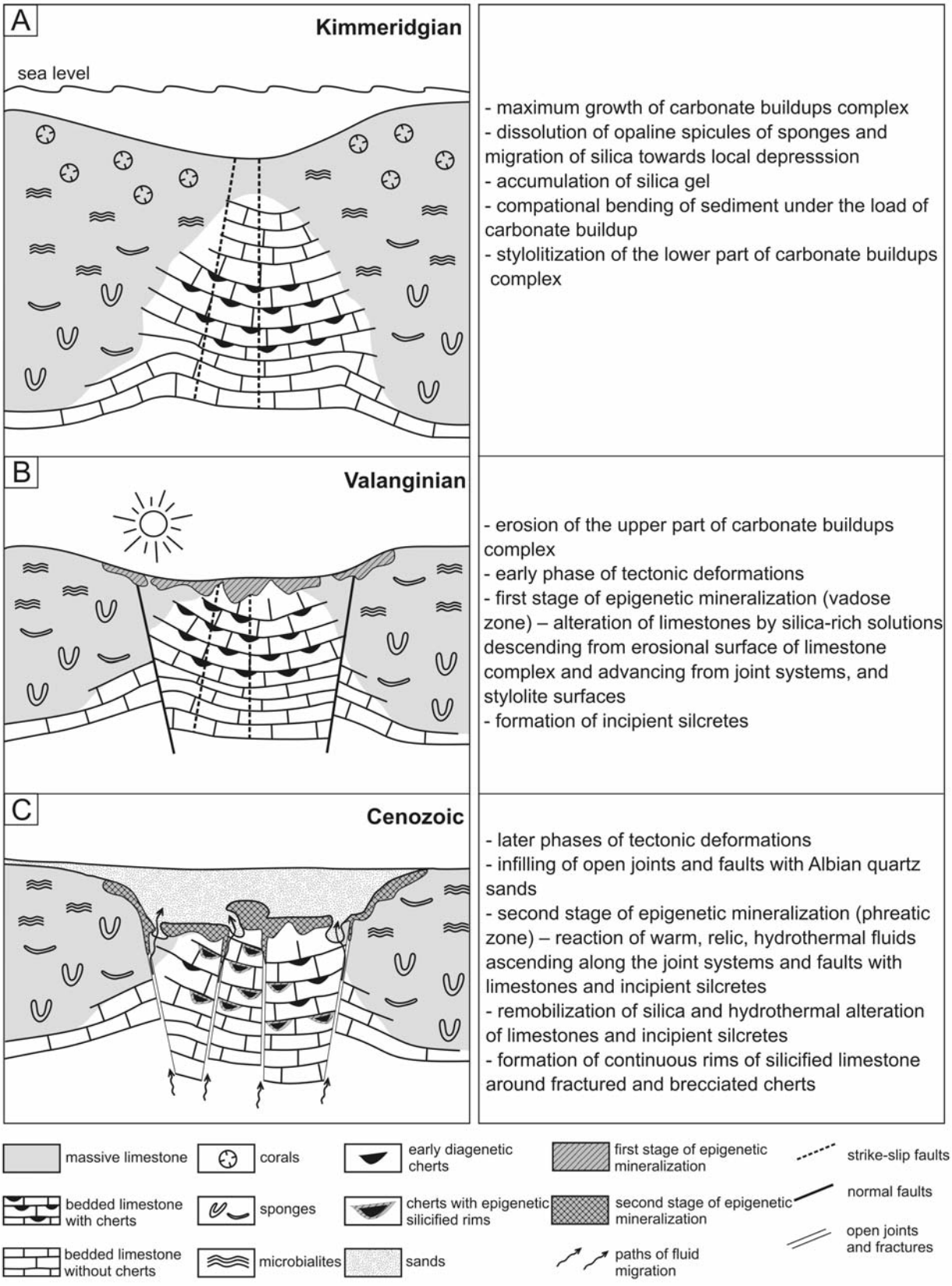

Text-fig. 15. Evolution model of epigenetic mineralization in Oxfordian limestones from the Sokole Hills (out of scale, other explanations in the text)

sands deposited on the silicified surface of the bedded limestones. The groundwater silcretes formed in a shallow, near-surface zone (cf. Ullyott and Nash 2006), under phreatic conditions, presumably close to the fluctuating zones of mixing of ascending solutions with groundwaters (Gradziński *et al*. 2011; cf. Thiry *et al*. 1988; Thiry 1997; Shaw and Nash 1998; Nash and Ullyott 2007; Bustillo *et al*. 2013). Silica leached from the Albian quartz sands might have migrated along the joints and faults (cf. Bukowy 1960; Caine *et al*. 1996; Ribeiro and Terrinha 2007) and might have precipitated on the silicified limestones and on the early diagenetic cherts (cf. Matyszkiewicz 1987), both acting as crystallization nuclei. The triggers of precipitation could have been, for example, fluctuations of pH or temperature in the mixing zone of ascending warm solutions and cold groundwaters.

The action of the ascending, warm solutions caused local dissolution of the unaltered limestones, visible especially within the Amphitheatre complex (Text-figs 4, 5A; cf. Gradziński *et al*., 2011), and modified the geochemistry of the existing silicified limestones. The silicification probably spread mainly through the zones in which Fe oxides and sulphides of metals had crystallized earlier. The recently observed porosity of the epigenetic silica accumulations presumably results from the dissolution of minute, unsilicified enclaves of limestone during the Cenozoic karstification and present day weathering or it could also be an effect of opal dehydration – a common feature described from silcretes (Azmon and Kedar 1985).

The age of the second stage of epigenetic silicification is open to question. In the nearby Gnaszyn area, situated some km west of Częstochowa, Barski and Ostrowski (2006), and Barski (2012) found neptunean dykes cutting through the Middle and Upper Jurassic strata that were filled with hydrothermal calcite mineralization. The orientation of the dykes corresponds to the regional fault pattern, and dinoflagellate cysts found in the dykes show that the opening of the fissures took place as early as the Kimmeridgian (Barski and Ostrowski 2006; Barski 2012). Gradziński *et al*. (2011) described from the Sokole Hills the spectacular, hypogenic caves formed during the Cenozoic, during the alteration of the Upper Jurassic limestones by ascending, warm solutions (cf. Palmer 1991; Andre and Rajaram 2005; Klimchouk 2007, 2009). Precipitation of silica on the brecciated, early diagenetic cherts acting as crystallization nuclei suggests that the second stage of epigenetic mineralization of the Oxfordian limestones also took place in the Cenozoic, after the last stages of deformation of the Upper Jurassic complex (Text-fig. 7).

Another, less likely possibility is stress concentration within the rims defining the transitional zones of partly silicified limestone that extend between the cherts and the unaltered limestone body hosting them, both showing different competence. The absence of cracks in the epigenetic silicified rims may result from rheological differences. Had the epigenetic silicification of the limestone taken place during the earlier stages of compression in the late Jurassic–early Cretaceous, simultaneous formation of fractures within the cherts would have resulted. Such fractures would have originated only within the cherts, as the bodies with greater competence than the less competent silicified rims and the limestone hosting them (cf. Sowers 1972).

The late stages of epigenetic mineralization of the limestones in the Sokole Hills could have developed as a result of multiple reactivations of old Palaeozoic faults and their propagation into the overlying Upper Jurassic strata. The tectonic activity in the study area was controlled by the adjacent, active KLFZ (Żaba 1999: cf. Sibson 1987). The alteration of Jurassic carbonates by hydrothermal solutions described from the southern part of the Kraków Upland (Matyszkiewicz 1987; Gołębiowska *et al*. 2010) is related to the rejuvenation of Palaeozoic dislocations of the KLFZ in the Savian phase of the Alpine orogeny (Oligocene/Miocene boundary). Similarly, the strong faulting of the Sokole Hills structure enabled the ascending mineralizing solutions to penetrate the Upper Jurassic complex.

The results of Nd isotope analyses of the mineralized limestones (Table 3) recalculated to T=23 Ma (Oligocene/Miocene boundary), i.e., corresponding to the age of the main faulting stage of the Upper Jurassic formation in the KCU and, probably, to the age of a new stage of epigenetic mineralization, range between –8.3 and –7.8, and do not reveal any significant contribution of mantle-sourced solutions (cf. Stille and Fischer 1990; Stille *et al*. 1989, 1996). Hence, the second stage of epigenetic mineralization presumably resulted from the action of warm, relict hydrothermal solutions ascending into the faulted, Upper Jurassic silicified limestones and into the Albian quartz sands covering them (Text-fig. 15C).

CONCLUSIONS

The epigenetic mineralization found in the Oxfordian bedded limestones from the Sokole Hills probably resulted from two different stages of the actions of solutions. During the first, Early Cretaceous stage, incipient silcretes formed under subtropical climatic

conditions at the erosional surface of the strongly denuded Upper Jurassic complex. These silcretes greatly hampered the first karstification phase of the Upper Jurassic carbonates, which began in the Hauterivian. The sources of silica for the microcrystalline quartz precipitated in the silcretes were descending, Si-rich, weathering solutions. Silicification altered not only the topmost part of the Upper Jurassic complex but mineralizing solutions percolated through the vadose zone much deeper into the bedded limestones along the joints and stylolites.

In the Albian, the opened joints and faults were filled with permeable quartz sands. During the second stage, which followed the Early Cretaceous tectonic activity, new dislocations were generated and opened. The joints and faults provided conduits for ascending, warm, relict hydrothermal solutions carrying Fe dioxides and metal sulphides, which partly dissolved the limestones and modified the chemical composition of the Lower Cretaceous incipient silcretes. Moreover, these solutions leached some silica from the Albian quartz sands filling the fissures and covering the top surface of the Jurassic limestones. Remobilized silica was then precipitated in the phreatic zone on the incipient silcretes and as rims on the brecciated, early diagenetic cherts, forming the groundwater silcretes. The precipitation of quartz on the brecciated cherts acting as crystallization nuclei indicates that the last stage of epigenetic silicification probably followed the final faulting stage of the limestone complex in the Cenozoic.

The bedded limestones are usually fine-detrital wackestones-packstones, cut by numerous stylolites, strongly fractured and faulted, which increases their susceptibility to epigenetic silicification. In contrast, the massive limestones forming the carbonate buildups are mostly boundstones, almost free of stylolites and poorly fractured, which greatly limits their alteration by invading siliceous solutions.

The multistage tectonic deformations affecting the bedded limestones since their early diagenesis were presumably related to periodical reactivations of the KFLZ dislocations cutting the Palaeozoic basement in the vicinity of the Sokole Hills.

Acknowledgements

The project was funded by the National Science Centre, on the basis of contract No. DEC-2011/03/B/ST10/06327, and from a statutory grant of the AGH University of Science and Technology. Authors would like to thank Z. Bełka for isotopic analyses and comments pertaining to interpretation of their results, and M. Wendorff for constructive remarks. We thank M. Bojanowski and an anonymous reviewer for critical reviews of the manuscript that helped to clarify several points.

REFERENCES

Alexandrowicz, S.W. 1960. Geological structure of the vicinity of Tyniec. *Biuletyn Instytutu Geologicznego*, **152**, 5–93. [In Polish with English summary]

Andre, B.J. and Rajaram, H. 2005. Dissolution of limestones fractures by cooling waters: Early development of hypogene karst systems. *Water Resources Research*, **41**, W01015 JAN 22 2005.

Aranburu, A., Fernández-Mendiola, P.A., López-Horgue, M.A. and Garcia-Mordéjar, J. 2002. Syntectonic hydrothermal calcite in a faulted carbonate platform margin (Albian of Jorrios, northern Spain). *Sedimentology*, **49**, 875–890.

Azmon, E. and Kedar, Y. 1985. Lower cretaceous silcrete-ferricrete at the Northern end of the African Tethys Shoreline, Maktesh Gadol, Israel. *Sedimentary Geology*, **43**, 261–276.

Barski, M. 2012. Dinoflagellate cysts from neptunian dykes in the Middle Jurassic of Poland – a stratigraphical approach. *Review of Palaeobotany and Palynology*, **169**, 38–47.

Barski, M. and Ostrowski S. 2006. Jurassic neptunian dykes. In: A. Wierzbowski, R. Aubrecht, J. Golonka, J. Gutowski, M. Krobicki, B.A. Matyja, G. Pieńkowski and A. Uchman (Eds), Jurassic of Poland and adjacent Slovakian Carpathians, Field trip guidebook of 7th International Congress on the Jurassic System, pp. 156–157. Warszawa.

Bednarek, J., Górecka, E. and Zapaśnik, T. 1985. Tectonically controlled development of ore mineralization in Jurassic sequence of the Silesian-Cracow Monocline. *Rocznik Polskiego Towarzystwa Geologicznego*, **53**, 43–62. [In Polish with English summary]

Braithwaite, C.J.R. 1989. Stylolites as open fluid conduits. *Marine and Petroleum Geology*, **6**, 93–96.

Bruhn, R.L., Parry, W.T., Yonkee, W.A. and Thompson, T. 1994. Fracturing and hydrothermal alteration in normal fault zones. *Pure and Applied Geophysics*, **142**, 609–644.

Bukowy, S. 1960. Notes on sedimentation and diagenesis of the Albian in Cracow region. *Biuletyn Instytutu Geologicznego,* **152**, 243–276. [In Polish with English summary]

Buła, Z. 2000. The lower palaeozoic of Upper Silesia and West Małopolska. *Prace Państwowego Instytutu Geologicznego*, **171**, 1–89. [In Polish]

Buła, Z. 2002. Geological Atlas of the Palaeozoic without the Permian in the border zone of the Upper Silesian and Małopolska Blocks. Explanatory text, pp. 1–28. Państwowy Instytut Geologiczny; Warszawa. [In Polish]

Buła, Z., Jachowicz, M. and Żaba, J. 1997. Principal char-

acteristics of the Upper Silesian Block and Małopolska Block border zone. *Geological Magazine*, **134**, 669–677.

Bustillo, M.A., Delgado, A., Rey, J. and Ruiz-Ortiz, P.A. 1998. Meteoric water participation in the genesis of Jurassic cherts in the Subbetic of southern Spain – a significant indicator of penecontemporaneous emergence. *Sedimentary Geology*, **119**, 85–102.

Bustillo, M.A., Plet, C. and Alonso-Zarza, A.M. 2013. Root calcretes and uranium-bearing silcretes at sedimentary discontinuities in the Miocene of the Madrid basin (Toledo, Spain). *Journal of Sedimentary Research*, **83**, 1130–1146.

Caine, J.S., Evans, J.P. and Forster, C.B. 1996. Fault zone architecture and permeability structure. *Geology*, **24**, 1025–1028.

Coimbra, R. Immenhauser, A. and Olóriz, F. 2014. Spatial geochemistry of Upper Jurassic carbonates (Iberian subplate). *Earth-Science Reviews*, **139**, 1–32.

Cornell, R.M. and Schwertmann, U. 2003. The iron oxides. Structure, properties, reactions, occurrence and uses, pp. 1–703. Wiley-VCH; Weinheim.

Czerniakowski, L.A., Lohmann, K.C., Wilson, J.L. 1984. Closed-system marine burial diagenesis: isotopic data from the Austin Chalk and its components. *Sedimentology*, **31**, 863–877.

Dadlez, R., Kowalczewski, Z. and Znosko, J. 1994. Some key problems of the pre-Permian tectonics of Poland. *Geological Quarterly*, **38**, 169–190.

Dixon, J.C. and McLaren, S.J. 2009. Duricrusts. In: A.J. Pearson and A.D. Abrahams (Eds), Geomorphology of desert environment, 123–152. Longman.

Dżułyński, S. 1952. The origin of the Upper Jurassic limestones in the Cracow area. *Rocznik Polskiego Towarzystwa Geologicznego*, **21**, 125–180. [In Polish with English summary]

Dżułyński, S. and Żabiński, W. 1954. Dark limestones in the Cracovian Jurassic sediments. *Acta Geologica Polonica*, **4**, 182–198. [In Polish with English summary]

Fanton, K.C., Holmden, C.E., Nowlan, G.S. and Haidl, F.M. 2002. $^{143}Nd/^{144}Nd$ and Sm/Nd stratigraphy of Upper Ordovician epeiric sea carbonates. *Geochimica et Cosmochimica Acta*, **66**, 241–255.

Franke, D. and Hoffmann, N. 1999. Das Elbe-Lineament-bedeutende Geofraktur oder Phantomgeblide? Teil 2, Regionale Zusammenhänge. *Zeitschrift für Geologische Wissenschaften*, **27**, 319–350.

Gaillard, C. 1983. Les biohermes à spongiaires et leur environment dans l'Oxfordian du Jura méridional. *Documents des Laboratoires de Géologie de la Faculté des Sciences de Lyon*, **90**, 1–515.

Garisson, R.E. 1981. Diagenesis of oceanic carbonate sediments: a review of the DSDP perspective. In: R.E. Warme, R.G. Douglas and E.L. Winterer (Eds), The Deep Sea Drilling Project: A Decade of Progress. *Special Publication of Society of Economic Paleontologists and Mineralogists*, **32**, 181–207.

Głazek, J. 1989. Paleokarts of Poland, In: D.C. Ford, J. Głazek and I. Horáček (Eds), Paleokarts a systematic and regional review, pp. 77–105. Akademia; Prague.

Głazek, J., Pacholewski, A. and Rożkowski, A. 1992. Karst aquifer of the Cracow-Wieluń Upland, Poland. In: W. Back, J.S. Herman and H. Paloc (Eds), Hydrogeology of selected karst regions. *International Contributions to Hydrogeology*, **13**, 289–306.

Gołębiowska, B., Pieczka, A., Rzepa, G., Matyszkiewicz, J. and Krajewski, M. 2010. Iodargyrite from Zalas (Cracow area, Poland) as an indicator of Oligocene-Miocene aridity in Central Europe. *Palaeogeography, Palaeoclimatology, Palaeoecology*, **296**, 130–137.

Górecka, E. and Zapaśnik, T. 1981. Epigenetic dolomites in Upper Jurassic rocks in the Silesian-Cracow Monocline. *Przegląd Geologiczny*, **10**, 529–532. [In Polish]

Gradziński, M., Motyka, J. and Górny, A. 2009. Artesian origin of a cave developed in an isolated horst: A case study of Smocza Jama (Kraków Upland, Poland). *Annales Societatis Geologorum Poloniae*, **79**, 159–168.

Gradziński, M., Hercman, H., Kicińska, D., Pura, D. and Urban, J. 2011. Ascending speleogenesis of Sokola Hill: a step towards a speleogenetic model of the Polish Jura. *Acta Geologica Polonica*, **61**, 341–365.

Gradziński, R. 1977. Sedimentation of "moulding sands" on karstified limestone surface in the middle part of Kraków Wieluń Upland. *Kras i Speleologia*, **1**, 59–70. [In Polish with English summary]

Gwinner, M.P. 1971. Carbonate rocks of the Upper Jurassic in SW-Germany. In: G. Müller (Ed.), Sedimentology of parts of Central Europe, pp. 193–207. Kramer; Frankfurt.

Heliasz, Z. 1980. Limestones silicification in the Julianka area, near Częstochowa. *Prace Naukowe Uniwersytetu Śląskiego w Katowicach*, **383**, Geologia, 92–101. [In Polish with English summary]

Heliasz, Z., Ptak, B., Więckowski, R. and Zieliński, T. 1982. Detailed geological map of Poland, 1:50 000, sheet Janów (846). Wydawnictwa Geologiczne; Warszawa. [In Polish]

Heliasz, Z., Ptak, B., Więckowski, R. and Zieliński, T. 1987. Explanation to detailed geological map of Poland sheet Janów (846) 1:50000, pp. 1–66. Wydawnictwa Geologiczne; Warszawa. [In Polish]

Jacobsen, S.B. and Wasserburg, G.J. 1980. Sm-Nd isotopic evolution of chondrites. *Earth and Planetary Science Letters*, **50**, 139–155.

James, V., Canerot, J., Meyer, A. Biteau, J.J. 2000. Growth and destruction of Bathonian silica nodules in the Western Pyrenees (France). *Sedimentary Geology*, **132**, 5–23.

Jones, C.E. and Jenkyns, H.C. 2001. Seawater strontium iso-

topes, oceanic anoxic events, and seafloor hydrothermal activity in the Jurassic and Cretaceous. *American Journal of Science*, **301**, 112–149.

Keupp, H., Koch, R. and Leinfelder, R.R. 1990. Steuerungsprozesse der Entwicklung von Oberjura-Spongiolithen Süddeutschland: Kenntnisstand, Probleme und Perspektiven. *Facies*, **23**, 141–174.

Klimchouk, A. 2007. Hypogene Speleogenesis. Hydrogeological and Morphogenetic Perspective, pp. 1–106. National Cave and Karst Institute; Carlsbad.

Klimchouk, A. 2009. Morphogenesis of hypogenic caves. *Geomorphology*, **106**, 100–117.

Knauth, L.P. 1979. A model for the origin of chert in limestone. *Geology*, **7**, 274–277.

Knauth, L.P. and Epstein, S. 1976. Hydrogen and oxygen isotope ratios in nodular and bedded cherts. *Geochimica et Cosmochimica Acta*, **40**, 1095–1108.

Kochman, A. and Matyszkiewicz, J. 2012. Microbial laminites with coprolites from Upper Jurassic carbonate buildups complex (Kraków-Częstochowa Upland; Poland). *Annales Societatis Geologorum Poloniae*, **82**, 331–347

Kochman, A. and Matyszkiewicz, J. 2013. Experimental method for estimation of compaction in the Oxfordian bedded limestones of the southern Kraków-Częstochowa Upland, Southern Poland. *Acta Geologica Polonica*, **63**, 681–696.

Kolodny, Y., Tarablous, A. and Frieslander, U. 1980. Participation of fresh water in chert diagenesis-evidence from stable isotopes and boron a-track mapping. *Sedimentology*, **27**, 305–316.

Kuźniar, W. and Żelechowski W. 1927. Materiały do poznania stosunku Karpat do ich przedgórza na przestrzeni do Morawskiej Ostrawy po Kraków. *Przegląd Górniczo-Hutniczy*, **19**, 327–334, 355–360, 393–402, 434–444, 465–471. [In Polish]

Lawrence, M.J.F. 1994. Conceptual model for early diagenetic chert and dolomite, Amuri Limestone Group, north-eastern South Island, New Zeland. *Sedimentology*, **41**, 479–478.

Leinfelder, R.R. 1993. Upper Jurassic reef types and controlling factors. *Profil*, **5**, 1–45.

Leinfelder, R.R. 1996. Distribution of Jurassic reef types: a mirror of structural and environmental changes during breakup of Pangea. *Canadian Society of Petroleum Geologists, Memoir*, **17**, 677–700.

Leinfelder, R.R., Krautter, M., Laternser, R., Nose, M., Schmid, D.U., Schweigert, G., Werner, W., Keupp, H., Brugger, H., Herrmann, R., Rehfeld-Kiefer, U., Schroeder, J.H., Reinhold, C., Koch, R., Zeiss, A., Schweizer, V., Christmann, H., Menges, G. and Luterbacher, H. 1994. The origin of Jurassic reefs: current research developments and results. *Facies*, **31**, 1–56.

Łaptaś, A. 1974. The dolomites in the Upper Jurassic limestones in the area of Cracow. *Rocznik Polskiego Towarzystwa Geologicznego*, **34**, 247–273. [In Polish with English summary]

Madsen, H.B., Stemmerik, L. and Sulryk, F. 2010. Diagenesis of silica-rich mound-bedded chalk, the Coniacian Arnager Limestone, Denmark. *Sedimentary Geology*, **223**, 51–60.

Maldonado, M., Carmona, C., Velasquez, Z., Puig, A., Cruzada, A., Lopez, A. and Young, C.M. 2005. Siliceous sponges as a silicon sink: an overlooked aspect of benthopelagic coupling in the marine silicon cycle. *Limnology and Oceanography*, **50**, 799–809.

Marcinowski, R. 1970a. The Cretaceous transgressive deposits east of Częstochowa (Polish Jura Chain). *Acta Geologica Polonica*, **20**, 413–449.

Marcinowski, R. 1970b. Turbidites in the Upper Oxfordian limestones at Jaskrów in the Polish Jura Chain. *Bulletin of the Polish Academy of Sciences, Earth Sciences*, **18**, 219–225.

Marcinowski, R. 1974. The transgressive Cretaceous (Upper Albian through Turonian) deposits of the Polish Jura Chain. *Acta Geologica Polonica*, **24**, 117–217.

Matyja, B.A. and Wierzbowski, A. 1992. Olsztyn, cyanobacteria-sponge biohermal complex; Oxfordian, Bifurcatus and Bimammatum zones. In: Oxfordian & Kimmeridgian joint working group meeting. International Subcommission on Jurassic Stratigraphy, pp. 35–37. Warszawa.

Matyja, B.A. and Wierzbowski, A. 1996. Sea-bottom relief and bathymetry of Late Jurassic sponge facies in Central Poland. *GeoResearch Forum*, **1-2**, 333–340.

Matyja, B.A. and Wierzbowski, A. 2006a. Open shelf facies of the Polish Jura Chain. In: A. Wierzbowski, R. Aubrecht, J. Golonka, J. Gutowski, M. Krobicki, B.A. Matyja, G. Pieńkowski and A. Uchman (Eds), Jurassic of Poland and adjacent Slovakian Carpathians, Field trip guidebook of 7th International Congress on the Jurassic System, pp. 198–199. Warszawa.

Matyja, B.A. and Wierzbowski, A. 2006b. Olsztyn, cyanobacteria-sponge biohermal complex; Upper Oxfordian (Bifurcatus and Bimmamatum zones). In: A. Wierzbowski, R. Aubrecht, J. Golonka, J. Gutowski, M. Krobicki, B.A. Matyja, G. Pieńkowski and A. Uchman (Eds), Jurassic of Poland and adjacent Slovakian Carpathians, Field trip guidebook of 7th International Congress on the Jurassic System, pp. 199–201. Warszawa.

Matyszkiewicz, J. 1987. Epigenetic silification of the Upper Oxfordian limestones in the vicinity of Kraków. *Annales Societatis Geologorum Poloniae*, **57**, 59–87. [In Polish with English summary]

Matyszkiewicz, J. 1989. Sedimentation and diagenesis of the Upper Oxfordian cyanobacterial-sponge limestones in Piekary near Kraków. *Annales Societatis Geologorum Poloniae*, **59**, 201–232.

Matyszkiewicz, J. 1994. Remarks on the deposition of pseudonodular limestones in the Cracow area (Oxfordian, Southern Poland). *Berliner Geowissenschaftliche Abhandlungen*, **E13**, 419–439.

Matyszkiewicz, J. 1999. Sea-bottom relief versus differential compaction in ancient platform carbonates: a critical reassessment of an example from Upper Jurassic of the Cracow-Wieluń Upland. *Annales Societatis Geologorum Poloniae*, **69**, 63–79.

Matyszkiewicz, J., Krajewski, M. and Żaba, J. 2006a. Structural control on the distribution of Upper Jurassic carbonate buildups in the Kraków-Wieluń Upland (South Poland). *Neues Jahrbuch für Geologie und Paläontologie, Monatshefte*, **3**, 182–192.

Matyszkiewicz, J., Krajewski, M. and Kędzierski, J. 2006b. Origin and evolution of an Upper Jurassic complex of carbonate buildups from Zegarowe Rocks (Kraków-Wieluń Upland, Poland). *Facies*, **52**, 249–263.

Matyszkiewicz, J., Kochman, A. and Duś, A. 2012. Influence of local sedimentary conditions on development of microbialites in the Oxfordian carbonate buildups from the southern part of the Kraków-Częstochowa Upland (south Poland). *Sedimentary Geology*, **263–264**, 109–132.

Migaszewski, Z.M., Gałuszka, A., Durakiewicz, T. and Starnawska, E. 2006. Middle Oxfordian – Lower Kimmeridgian chert nodules in the Holy Cross Mountains, south-central Poland. *Sedimentary Geology*, **187**, 11–28.

Milnes, A.R. and Thiry, M. 1992. Silcretes. In: Martini, I.P., Chesworth, W. (Eds), Weathering, soils and palaeosols, pp. 349–377. Elsevier; Amsterdam.

Mišik, M. 1996. Silica spherulites and fossil silcretes in carbonate rocks of the Western Carpathians. *Geologica Carpathica*, **47**, 91–105.

Morawska, A. 1997. The Lubliniec Fracture Zone: boundary of the Upper Silesia and Malopolska Massifs, southern Poland. *Annales Societatis Geologorum Poloniae*, **67**, 429–437.

Morozewicz, J. 1909. O haczetynie i jego Bonarskim złożu. *Kosmos*, **34**, 610–624.

Murata, K.J. and Norman, M.B. 1976. An index of crystallinity for quartz. *American Journal of Science*, **276**, 1120–1130.

Nash, D.J. and Ullyott, J.S. 2007. Silcrete. In: D.J. Nash and S.J. McLaren (Eds), Geochemical sediments and landscapes, pp. 95–143. Blackwell; Oxford,

Nash, D.J., Shaw, P.A. and Ullyott, J.S. 1998. Drainage-line silcretes of the Middle Kalahari: an analogue for Cenozoic sarsen trains? *Proceedings of the Geologists' Association*, **109**, 241–254.

Neuweiler, F., Daoust, I., Bourque P.-A. and Burdige, D.J. 2007. Degradative calcification of a modern siliceous sponge from the Great Bahama Bank, the Bahamas: a guide for interpretation of ancient sponge-bearing limestones. *Journal of Sedimentary Research*, **77**, 552–563.

Ni, S., Ju, Y., Hou, Q., Wang, S., Liu, Q., Wu, Y. and Ziao, L. 2009. Enrichment of heavy metal elements and their adsorption on iron oxides during carbonate rock weathering. *Progress in Natural Science*, **19**, 1133–1139.

Palmer, A.N. 1991. Origin and morphology of limestone caves. *Geological Society of America Bulletin*, **103**, 1–21.

Pin, C., Briot, D., Bassin, C. and Poitrasson, F. 1994. Concomitant separation of strontium and samarium-neodymium for isotopic analysis in silicate samples, based on specific extraction chromatography. *Analytica Chimica Acta*, **298**, 209–217.

Pouchou, J.L. and Pichoir, F. 1985. "PAP" (φ-ρ-Z) procedure for improved quantitative microanalysis. In: J.T. Armstrong (Ed.), Microbeam Analysis, pp. 104–106. San Francisco Press; San Francisco,

Pucéat, E., Lécuyer, C. and Reisberg, L. 2005. Neodymium isotopic evolution of the Western Tethyan seawater throughout the Cretaceous. *Earth and Planetary Science Letters*, **236**, 705–720.

Pulina, M., Żaba, J. and Polonius, A. 2005. Relation between karst forms of Smoleń-Niegowonice Range and tectonic activity of Cracow-Wieluń Upland. *Kras i Speleologia*, **11**, 39–85. [In Polish with English summary]

Rajchel, J. 1970. Badania sedymentologiczne krzemieni jurajskich pod Krakowem. *Sprawozdania z Posiedzeń Komisji Oddziału Polskiej Akademii Nauk w Krakowie*, **14**, 625–645. [In Polish]

Ribeiro, C. and Terrinha, P. 2007. Formation, deformation and chertification of systematic clastic dykes in a differentially lithified carbonate multilayer. SW Iberia, Algarve Basin, Lower Jurassic. *Sedimentary Geology*, **196**, 201–215.

Riding, R. 2002. Structure and composition of organic reefs and carbonate mud mounds: concepts and categories. *Earth-Science Reviews*, **58**, 163–231.

Rongemaille, E., Bayon, G., Pierre, C., Bollinger, C., Chu, N.C., Fouquet, Y., Riboulot, V. and Voisset, M. 2011. Rare earth elements in cold seep carbonates from the Niger delta. *Chemical Geology*, **286**, 196–206.

Różycki, S.Z. 1937. Alb, cenoman i turon w okolicy stacji Złoty Potok (koło Koniecpola). *Sprawozdania Państwowego Instytutu Geo1ogicznego*, **9**, 19–57. [With German summary]

Rühle, E., Ciuk, E., Osika, R. and Znosko, J. 1977. Geological Map of Poland without Quaternary deposits, scale 1 : 500 000. Wydawnictwa Geologiczne; Warszawa. [In Polish]

Scheinost, A.C. and Schwertmann, U. 1999. Color identification of iron oxides and hydroxysulfates: use and limitations. *Soil Science Society of America Journal*, **63**, 1463–1471.

Schlanger, S.O. and Douglas, R.G. 1974. The pelagic

oozechalk-limestone transition and its implications for marine stratigraphy. In: K.J. Hsü and H.C. Jenkyns (Eds), Pelagic Sediments. *Special Publication of the International Association of Sedimentologists*, **1**, 117–148.

Shaw, P.A. and Nash, D.J. 1998. Dual mechanisms for the formation of fluvial silcretes in the distal reaches of the Okavango Delta Fan, Botswana. *Earth Surface Processes and Landforms*, **23**, 705–714.

Sibson, R.H. 1987. Earthquake rupturing as a hydrothermal mineralizing agent. *Geology*, **15**, 701–704.

Sowers, G.M. 1972. Theory of spacing of extension fractures. In: H. Pincus (Ed.), Geological factors in rapid excavagation. *Bulletin of the Geological Society of America*, *Engeneering Geology case history*, **9**, 27–53.

Stille, P. and Fisher, H. 1990. Secular variation in the isotopic composition of Nd in Tethys seawater. *Geochimica and Cosmochimica Acta*, **54**, 3139–3145.

Stille, P., Clauer, N. and Abrecht, J. 1989. Nd isotopic composition of Jurassic Tethys seawater and the genesis of Alpine Mn-deposits: Evidence from Sr-Nd isotope data. *Geochimica and Cosmochimica Acta*, **53**, 1095–1099.

Stille, P., Steinmann, M. and Riggs, S.R. 1996. Nd isotope evidence for the evolution of the paleocurrents in the Atlantic and Tethys Oceans during the past 180 Ma. *Earth and Planetary Science Letters*, **144**, 9–19.

Thiry, M. 1997. Continental silicification: a review. In: H. Paquet and N. Clauer (Eds), Soils and sediments: mineralogy and geochemistry, pp. 191–221. Springer; Berlin.

Thiry, M. 1999. Diversity of continental silicification features: examples from the Cenozoic deposits in the Paris Basin and neighbouring basement. In: M. Thiry and R. Simon-Coinçon (Eds), Palaeoweathering, Palaeosurfaces and Related Continental Deposits, International Association of Sedimentologists, *Special Publication*, **27**, 87–127.

Thiry, M., Bertrand-Ayrault, M. and Grisoni, J.C. 1988. Ground-water silicification and leaching in sands: example of the Fontainebleau Sand (Oligocene) in the Paris Basin. *Bulletin of the Geological Society of America*, **100**, 1283–1290.

Thiry, M. and Milnes, A.R. 1991. Pedogenic and groundwater silcretes at Stuart Creek opal field, South Australia. *Journal of Sedimentary Petrology*, **61**, 111–127.

Thiry, M. and Simon-Coinçon, R. 1996. Tertiary palaeoweatherings and silcretes in the southern Paris Basin. *Catena*, **26**, 1–26.

Tofalo, O.R. and Pazos, P.J. 2010. Paleoclimatic implications (Late Cretaceous-Paleogene) from micromorphology of calcretes, palustrine limestones and silcretes, southern Parana Basin, Uruguay. *Journal of South American Earth Sciences*, **29**, 665–675.

Trammer, J. 1982. Lower to Middle Oxfordian sponges of the Polish Jura. *Acta Geologica Polonica*, **32**, 1–39.

Tyc, A. 2009. Hypogenic ascending speleogenesis in the Kraków-Częstochowa Upland (Poland) – Evidence in cave morphology and surface relief. In: A. Klimchouk and D. Ford (Eds), Hypogene Speleogenesis and karst Hydrology of Artesian basin. *Special Paper*, **1**, 201–208.

Ullyott, J.S. and Nash, D.J. 2006. Micromorphology and geochemistry of groundwater silcretes in the eastern South Downs, UK. *Sedimentology*, **53**, 387–412.

Urban, J. and Gradziński, M. 2004. Traditions and perspec tives of protection of "Sokole Góry" nature reserve. In: J. Partyka (Ed.), Zróżnicowanie i przemiany środowiska przyrodniczo-kulturowego Wyżyny Krakowsko-Częstochowskiej, Przyroda, pp. 89–95. Ojców. [In Polish with English summary]

Wójcik, Z. 2004. On the history of calcareous spar mining in Małopolska Upland. In: J. Partyka (Ed.), Zróżnicowanie i przemiany środowiska przyrodniczo-kulturowego Wyżyny Krakowsko-Częstochowskiej, Kultura, pp. 345–350. Ojców. [In Polish with English summary]

Żaba, J. 1999. The structural evolution of Lower Palaeozoic succession in the Upper Silesia Block and Małopolska Block border zone, southern Poland. *Prace Państwowego Instytutu Geologicznego*, **166**, 1–162. [In Polish with English summary]

Żaba, J. and Tyc A. 2007. Tectonic and karst phenomena of the Ogrodzieniec Area. In: P. Socha, K., Stefaniak and A. Tyc (Eds), Karst and Cryokarst. Guidebook & Abstracts, 25th Speleological School, 8th GLACKIPR Symposium, pp. 120–121. Sosnowiec–Wrocław.

Żelaźniewicz, A., Aleksandrowski, P., Buła, Z., Karnkowski, P.H., Konon, A., Oszczypko, N., Ślączka, A., Żaba, J. and Żytko, K. 2011. Tectonic subdivision of Poland, 60 pp. Komitet Nauk Geologicznych Polskiej Akademii Nauk; Wrocław. [In Polish]

Manuscript submitted: 15th October 2014
Revised version accepted: 10th April 2015